

Summer melt rates on Penny Ice Cap, Baffin Island: Past and recent trends and implications for regional climate

Christian Zdanowicz,¹ Anna Smetny-Sowa,² David Fisher,¹ Nicole Schaffer,³ Luke Copland,³ Joe Eley,⁴ and Florent Dupont^{5,6}

Received 17 October 2011; revised 23 January 2012; accepted 6 February 2012; published 10 April 2012.

[1] At latitude 67°N, Penny Ice Cap on Baffin Island is the southernmost large ice cap in the Canadian Arctic, yet its past and recent evolution is poorly documented. Here we present a synthesis of climatological observations, mass balance measurements and proxy climate data from cores drilled on the ice cap over the past six decades (1953 to 2011). We find that starting in the 1980s, Penny Ice Cap entered a phase of enhanced melt rates related to rising summer and winter air temperatures across the eastern Arctic. Presently, 70 to 100% (volume) of the annual accumulation at the ice cap summit is in the form of refrozen meltwater. Recent surface melt rates are found to be comparable to those last experienced more than 3000 years ago. Enhanced surface melt, water percolation and refreezing have led to a downward transfer of latent heat that raised the subsurface firn temperature by 10°C (at 10 m depth) since the mid-1990s. This process may accelerate further mass loss of the ice cap by pre-conditioning the firn for the ensuing melt season. Recent warming in the Baffin region has been larger in winter but more regular in summer, and observations on Penny Ice Cap suggest that it was relatively uniform over the 2000-m altitude range of the ice cap. Our findings are consistent with trends in glacier mass loss in the Canadian High Arctic and regional sea-ice cover reduction, reinforcing the view that the Arctic appears to be reverting back to a thermal state not seen in millennia.

Citation: Zdanowicz, C., A. Smetny-Sowa, D. Fisher, N. Schaffer, L. Copland, J. Eley, and F. Dupont (2012), Summer melt rates on Penny Ice Cap, Baffin Island: Past and recent trends and implications for regional climate, *J. Geophys. Res.*, 117, F02006, doi:10.1029/2011JF002248.

1. Introduction

[2] Outside of Greenland, the Canadian Arctic Archipelago (CAA) holds the largest total area of land ice (~150,000 km²) in the north circumpolar region. Recent studies have revealed increasing rates of ice mass wastage in the CAA over the past ~15–20 years, making this region one of the largest contributors to present sea-level rise after Greenland and Antarctica [Sharp *et al.*, 2011; Fisher *et al.*, 2011; Gardner *et al.*, 2011; Radić and Hock, 2011; Jacob *et al.*, 2012]. The increased glacier losses are linked to a warming trend observed in both summer and winter across the entire eastern Arctic (Environment Canada, Climate trends and variations bulletin, 2010, www.ec.gc.ca/adsc-cmda, hereinafter

referred to as Environment Canada, online bulletin, 2010). The best documented evidence for the recent glacier mass loss comes from the Queen Elizabeth Islands (QEI), north of Lancaster Sound [e.g., Gardner *et al.*, 2011]. Reliable observations, short or long, are comparatively scarce for Baffin Island [e.g., Jacob *et al.*, 2012], even though this region contains almost a third of all glacier-covered land in the CAA. The scarcity of observations from Baffin Island makes it difficult to compare regional responses of the cryosphere to Arctic warming.

[3] Located at latitude 67°N, Penny Ice Cap (Figure 1) is the southernmost of the large Canadian Arctic ice caps, and the only one on Baffin Island that rises to a sufficient altitude (~1930 m at its highest point) for a firn zone to persist. Barnes Ice Cap, some 400 km further north, accumulates as superimposed ice only [Baird, 1952], as do the smaller ice-fields on Meta Incognita Peninsula to the south [Blake, 1953; Zdanowicz, 2007]. Barnes and Penny Ice Caps are partial remnants of the Laurentide Ice Sheet, and late glacial ice layers are preserved near their bed [Zdanowicz *et al.*, 2002]. The presence of a firn zone on Penny Ice Cap has allowed paleoclimatic information to be preserved and recovered by coring [Fisher *et al.*, 1998], making it possible to place recent observations from this ice cap in a centennial to millennial perspective. In this paper, we present a synthesis of past and recent observations from Penny Ice Cap

¹Geological Survey of Canada, Natural Resources Canada, Ottawa, Ontario, Canada.

²Department of Earth Sciences, University of Western Ontario, London, Ontario, Canada.

³Department of Geography, University of Ottawa, Ottawa, Ontario, Canada.

⁴6 Sullivan St., Saskatoon, Saskatchewan, Canada.

⁵Centre d'Applications et de Recherches en Télédétection, Université de Sherbrooke, Quebec, Canada.

⁶Laboratoire de Glaciologie et Géophysique de l'Environnement, UMR 5183, UJF-CNRS, Grenoble F-38041, France.

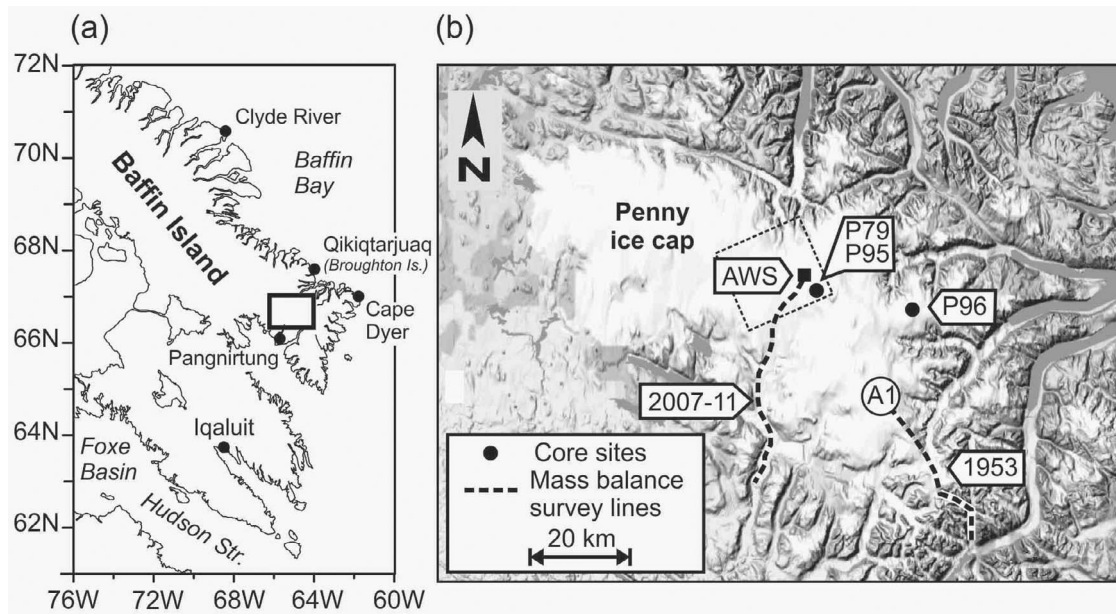


Figure 1. (a) Map of southern Baffin Island, Nunavut, showing location of study area (framed) and of weather monitoring stations mentioned in the text. (b) Map of Penny Ice Cap showing the surface mass balance stake lines (dotted lines; 1953 and 2007–11), the location of the automated weather station (AWS), and the ice-coring sites (P79, P95, P96) discussed in the text. The stippled square at the ice cap summit defines the pixel footprint of spaceborne passive microwave observations used to estimate changes in the melt season duration, as described in the text.

based on historical records, ice-core data, surface mass balance measurements, firn temperature soundings, satellite observations and climatological data. We use these various documentary sources to identify past and recent trends in summer melt rates on the ice cap, and examine the implications for glacier mass balance and regional climate. Our goal is to establish a framework of reference for ongoing assessments of the present and future evolution of Penny Ice Cap using in situ and remotely-sensed observations [Schaffer *et al.*, 2011].

2. Data Sets and Methods

2.1. Historical Records

[4] The first scientific expedition to Penny Ice Cap was carried out by the Arctic Institute of North America (AINA) in the summer of 1953 [Baird, 1953]. It conducted glaciological and climatological observations at various sites on the ice cap, including snow and ice stratigraphy and density, summer melt progression, surface mass balance and energy budget. Detailed methods and findings were reported by Ward [1954], Ward and Baird [1954], and Orvig [1954]. Later in 1979, a reconnaissance study was made to evaluate the potential to recover a deep ice-core climate record from Penny Ice Cap summit. As part of this study, a 20-m core was recovered and firn temperatures were measured in the borehole [Holdsworth, 1984]. We use these data, as well as the AINA expedition records, to place recent observations from the ice cap in historical context.

2.2. Firn and Ice Cores

[5] Cores were recovered from the summit region of Penny Ice Cap in 1953, 1979, 1995, 1996, 2010 and 2011

(Figure 1). The 1953 core [Ward, 1954] was drilled to a depth of 21 m at a site (A1) located at the southeast end of the summit ridge. The exact altitude of this site is uncertain (see section 3.4. below) but is thought to be ~ 1930 m. In 1979 a 20-m core was retrieved from a site (P79) at 175 m [Holdsworth, 1984]. Subsequently, two deeper cores were recovered by a Canadian-American-Japanese consortium in 1995 and 1996. The first and longer of these cores was drilled at a site (P95) located near the P79 borehole, at an altitude of 1860 m. The P95 borehole reached bedrock at a depth of 334 m. The second deep core was drilled to a depth of 176 m from a site (P96) 30 km E of P95 at an altitude of 1810 m. The climate records developed from the P95 and P96 deep cores extend back to the last glacial period, more than 11.5 ka before present (b.p.), although discontinuities may exist in the early Holocene [Fisher *et al.*, 1998; Okuyama *et al.*, 2003]. In 2010 and 2011, shallow firn cores were obtained to update the paleoclimate records developed from the 1995 core. A 23-m core (P2010) was hand-drilled in May 2010 at the location of the P95 borehole. A shorter, 5.5-m core was obtained in May 2011 a few km away at a similar altitude.

[6] In this paper, we use the ice-core data to estimate historical trends in summer melt on Penny Ice Cap. Each summer, surface melt in the accumulation area causes meltwater to percolate and refreeze into underlying, colder firn layers. The resulting infiltration ice forms distinct horizontal layers, but also irregular horizontal and vertical features such as ice glands, lenses and pipes. We refer collectively to these as “melt features”, abbreviated MF. The number and thickness of MF in the firn layers of ice caps can be positively correlated with past summer warmth [Koerner, 1977; Fisher *et al.*, 2011]. Summer-winter temperature

contrast, and the timing and duration of the melt period are also determining factors in MF formation [Pfeffer and Humphrey, 1998; Bell et al., 2008]. Melt feature records were previously developed from the cores drilled in 1995 (P95) and 1996 (P96) at Penny Ice Cap summit (Figure 1). The stratigraphy of the P95 core was described and logged by the late R. Koerner [Grumet et al., 2001]. Owing to microfractures in the core, the proper identification of MF was limited to depths < 245 m, or back to ~2 ka b.p. The stratigraphy of the P96 core was described by Okuyama et al. [2003].

[7] For the present study, the firm core drilled in 2010 was measured for MF, density, and solid electrical conductivity (ECM) [Hammer, 1980]. These data were used to correlate the new 2010 core with the older P95 record (Appendix A). The 5.5-m firm core drilled in 2011 extended this composite MF record by one year (to 2010). Because ice-core density measurements are discontinuous, we report the percentage of MF in volume, rather than mass terms. For any time interval of length N (years) in the composite record, the MF content is expressed as the volumetric percentage of the core occupied by ice, following:

$$MF = \frac{\sum(dZ_{MF}) + \sum(dZ_F F_{ice})}{\bar{N}\bar{A}} \times 100 \quad (1)$$

where dZ_{MF} is the thickness of individual MF in the core section, dZ_F is the thickness of firm layers, F_{ice} gives the volumetric fraction of refrozen meltwater in the firm layers, and \bar{A} is the mean ice accumulation rate. The ice content in the “icy firm” layers was estimated from their density and was found to average $5 \pm 5\%$. This value of F_{ice} also gave the best visual agreement between the ~15-year overlapping sections of the 1995 and 2010 MF records. In the deeper parts of the P95 core, the MF data were corrected to account for ice layer thinning. See Appendix A and B, and Fisher et al. [2011] for additional details on the development of MF records.

2.3. Automated Weather Station Data

[8] Two automated weather stations (AWSs) have operated at the summit of Penny Ice Cap (Figure 1). The first AWS was installed in May 1992 and remained in operation until July 2000 [Jacobs, 1990; Eley, 2001]. It recorded hourly and daily air and firm temperatures over a range of heights and depths, as well as snow surface height, relative humidity, wind speed and direction, and total incoming solar radiation. In 2007, another, simpler AWS was set up at the same site to record air temperature and snow surface height changes. Of special relevance to this study are measurements of firm temperature and snow surface height. The firm temperatures between 1994 and 2000 were measured using a thermistor string buried in the firm. The thermistors (type YSI 4403, 1 k Ω half-bridge) were spaced on the cable at intervals of a few meters. The cable was gradually buried by snow and firm accumulation, such that the maximum depth of the measurements increased from 6.2 m in May 1992, to 13.1 m in July 2000 when the AWS was removed. Eley [2001] interpolated these data to produce homogeneous time series of firm temperature at fixed depth intervals.

In April 2011, a new thermistor cable (RST Instruments, Coquitlam, B.C.) was installed and connected to the AWS erected in 2007. This cable is equipped with the same type of thermistors as on the earlier AWS, spaced at 1-m intervals, with the deepest buried at a depth of 10.5 m. In both periods of record (1992–2000 and 2007–11), inter-seasonal changes in snow surface height were measured with an ultrasonic distance gauge (UDG; model SR50, Campbell Scientific Canada, Edmonton) mounted on a cross-arm at a height of several meters.

2.4. Climatological Records

[9] To help place and interpret observations from Penny Ice Cap in a regional climatic context, we used archived climatological data from the eastern Canadian Arctic available from Environment Canada. Temperature and precipitation records are available from 15 different weather monitoring stations in the southern Baffin Island region. While some of these records extend back to the 1930s, most of them are much shorter (<30 years) and/or discontinuous. In this paper, we used records from a few stations only (Figure 1) selected for their length and/or proximity to Penny Ice Cap. These are records from Pangnirtung (N 66.15°; W 67.72°), Qikiqtarjuaq (formerly Broughton Island; N 67.55°; W 64.03°), Clyde River (N 70.48°; W 65.52°) and Cape Dyer (N 66.55°; W 64.03°). In addition, we used seasonal temperature and annual precipitation anomalies for the eastern Canadian Arctic region produced by Environment Canada (online bulletin, 2010). This region corresponds to the “Arctic Mountains and Fjords” climatological region as defined by Environment Canada, which comprises the mountainous eastern sectors and coastlines of Baffin, Bylot, Devon and Ellesmere Islands facing Baffin Bay and Nares Strait. The climatological anomaly series used in this study were computed by interpolation of individual station data, as described by Milewska and Hogg [2001] and Fritzsche [2011]. Most usable station records for this region are in fact located on eastern Baffin Island. We use these regional anomalies rather than data from individual Baffin climate stations, because records from the latter are too often discontinuous. Furthermore, interannual temperature variations are typically synchronous across the Baffin region [Jacobs and Newell, 1979].

[10] To characterize present-day air temperature lapse rates over Penny Ice Cap, we compared air temperature recordings from the AWS at Penny Ice Cap summit (periods 1992–2000 and 2007–2011) with archived weather station data from Qikiqtarjuaq and Clyde River on the Baffin Bay coast. For comparison, we also computed the mean July air temperature lapse rate for 1953, using data from Orvig’s [1954] report of the AINA summer expedition, and 1953 weather station records from Cape Dyer.

2.5. Field Measurements of Surface Mass Balance

[11] In 2007, a program to evaluate and monitor the mass balance of Penny Ice Cap was initiated by the Geological Survey of Canada in collaboration with Parks Canada Agency. Initially, and up to 2010, the program of observations was limited to in situ measurements of surface accumulation and ablation. The measurements are performed once a year, in early to mid-April, with ski-equipped aircraft

and snowmobile support. Several lines of reference stakes have been set on the ice cap, at intervals of a few km or ~ 100 m of altitude difference. The most complete data set, presented in this paper, comes from a line of 20 stakes installed on the western slopes of Penny Ice Cap, from the summit area (~ 1860 m) down to the terminus of an unnamed glacier outlet (~ 350 m; Figure 1). The surface altitude on this transect was measured in May 2011 with a high-precision Trimble R7 differential GPS system (Trimble Navigation Ltd., Sunnyvale, CA). The data were post-processed with the Precise Point Positioning service (Natural Resources Canada, Precise Point Positioning (PPP) service, http://webapp.csrns.nrcan.gc.ca/index_e/products_e/services_e/ppp_e.html, 2011) and have an estimated vertical accuracy of ± 0.1 m. For mass balance measurements, we use the so-called glaciological method, in which the net firm/ice accumulation (winter) or net loss (summer) are estimated from measured changes in the exposed length of the stakes [Østrem and Brugman, 1991]. At each stake, the snowpack stratigraphy is also recorded and the density profile measured, and multiple soundings are made with a probe over an area of ~ 10 m² to obtain the mean snow thickness. Presently, our in situ mass balance measurements on Penny Ice Cap do not account for internal accumulation, because of the extreme difficulty of quantifying meltwater percolation in firn (see section 3.2 below). In agreement with recommended usage [Cogley et al., 2011], we use the term *surface mass balance* (abbreviated SBM, or \dot{b}) to report our mass balance estimates from individual stakes. For fall and winter accumulation estimated from snowpits, we use the term winter (surface) balance b_w .

2.6. Passive Microwave Brightness Temperatures

[12] To supplement AWS data and climatological records, we estimated changes in the duration of surface melt on Penny Ice Cap over the period 1979–2010 using passive measurements of snow microwave brightness temperature T_b from satellites. This method is founded on the assumption that abrupt changes in T_b detected on the ice cap surface at the onset and end of the melt season are due to changes in the snowpack liquid water content, which strongly affects the microwave emissivity e of the snow [Zwally and Fiegles, 1994; Ashcraft and Long, 2006]. In this study, we used an algorithm developed by Dupont et al. [2011] that uses combined gridded passive microwave data from two spaceborne instruments: (1) the Nimbus-7 Scanning Multichannel Microwave Radiometer (SMMR), for the period from 1979–1986 [Knowles et al., 2002]; and (2) the Defense Meteorological Satellite Program-Special Sensor Microwave/Imager (DMSP SSM/I) for the period 1987–2010 [Maslanik and Stroeve, 2011]. The algorithm sets a threshold separating the winter (dry) and summer (wet) modes of brightness temperatures, and then calculates the number of days above this threshold to derive the annual period of melt duration. In this study, the method was applied to a single grid pixel with a footprint of 25×25 km at the summit of the ice cap (Figure 1), because surrounding pixels extended beyond the ice-covered area or overlapped with nunataks or water bodies. Conveniently, the P95 ice-coring site is located within the boundaries of this pixel. The time series of surface melt duration derived by the microwave brightness temperature can therefore be compared with the

summer melt intensity series inferred from the extended P95 ice-core record.

3. Results

3.1. General Setting

[13] Located on the highlands of Cumberland Peninsula, Penny Ice Cap (N 67.27°; W 65.85°) covers an area of 6410 km², and an altitude range of ~ 1980 m from the terminus of Coronation Glacier, which calves into Baffin Bay, to the highest point on the central ice divide. Previous studies [Ward, 1954; Holdsworth, 1984] and recent field observations (snow pits and firn cores) indicate that most of the accumulation area on the ice cap (above ~ 1500 m) is in the percolation facies. Snow that accumulates in the cold months melts partly or completely in summer, and the meltwater percolates through underlying firn to refreeze as bubble-poor infiltration ice. At altitudes between 1500 and 1700 m there is some accumulation in the form of superimposed ice. The present-day accumulation area to total area ratio (AAR) of the ice cap, estimated using a digital elevation model, is ~ 0.3 [Schaffer et al., 2011]. The present-day mean annual temperature (MAT) at the ice cap summit, estimated from AWS recordings (1992–2000; 2007–11) is $-16 \pm 1.5^\circ\text{C}$. The regional climate is wet for the Arctic, with total precipitation exceeding 300 mm a⁻¹ (water equivalent) at nearby climate stations on the Baffin Bay coast [Maxwell, 1981]. The relative humidity over the ice cap frequently exceeds 90% in both summer and winter. Snow accumulates mostly in autumn (late August to mid-November) and to a lesser extent in spring (late March to May) with the frequent passage of cyclones tracking north-northeast across or around southern Baffin Island [Bradley, 1973; Maxwell, 1981; Sorterberg and Walsh, 2008; Sepp and Jaagus, 2010]. The annual thickness of the snow cover measured in late winter at the summit of Penny Ice Cap is presently ~ 1 – 1.2 m, with a mean density of 350 kg m⁻³, and the mean ice accumulation rate \bar{A} , inferred from ice-core data, is 0.37 ± 0.5 m a⁻¹ (0.34 m a⁻¹ water equivalent). The ice cap straddles the Arctic circle (66°N) and experiences up to 20 hours of daylight during the melt season from early June to mid-August, although the total sunshine actually received at the surface is typically less ($\sim 26\%$ of maximum) owing to frequent low cloud cover [Orvig, 1954].

3.2. Historical Trends in Summer Melt

[14] Previously, Holdsworth [1984] had found that MF % in a 20-m core (P79) drilled at Penny Ice Cap summit were well correlated with mean maximum daily July air temperatures recorded at Broughton Island ($R = 0.553$) and Cape Dyer ($R = 0.563$) on the Baffin Bay coast (period 1958–1979; using 5-year running means of the data series). More recent thermistor data (see section 3.3 below) reveal that the firn at Penny Ice Cap summit commonly becomes isothermal at 0°C in summer (July) to a depth exceeding 1 m, i.e. greater than the mean depth of the annual snowpack. Meltwater can therefore percolate into firn from previous years, and this can occur even in the presence of ice layers [Ward, 1954; Orvig, 1954]. Evidence of deep percolation was observed in the ion chemistry profiles of snowpits and the P95 and P96 ice cores, where “washed-out” sections due to

elution, sometimes >2 m, occurred irregularly [Goto-Azuma *et al.*, 2002]. Owing to this effect, MF in the firn could be offset by 1–5 years relative to the accumulation sequence. Hence, MF % variations are not expected to faithfully track annual summer temperature variations, but should generally follow multi-annual or decadal trends. The spatial continuity of MF in firn is also irregular, although thick ice layers (>0.1 m, formed in years of high summer melt) can be followed laterally over hundreds of meters. For these reasons, trends in the MF records are typically examined through time-averaging windows of 5 years or more [e.g., Kameda *et al.*, 1995; Fisher *et al.*, 2011]. The longer the time-averaging window, the more robust the trends (if any). Derivation of error estimates for the ice-core MF record are presented in Appendix B.

[15] Figure 2a shows the composite MF % record for Penny Ice Cap summit over the period 1945–2010, displayed as anomalies relative to the mean of the years 1961–1990 conventionally used for climatological data. The MF averaged 61% for the entire 65-year period and also for the interval 1961–1990, but the mean of the past 15 years [1995–2010] has risen to 72%, with individual years recording 100% of accumulation as infiltration ice. Figures 2b and 2c show that both summer and winter air temperatures in this region have risen markedly over the same period. The rise in summer temperatures has been steadier, but recent positive winter temperatures anomalies are twice as large ($\sim 4^{\circ}\text{C}$) as summer anomalies ($\sim 2^{\circ}\text{C}$). The MF in Penny Ice Cap cores generally track summer temperature variations, except for a period of a few years between 2003 and 2006 when the MF % apparently declined while summer temperatures rose or were stable. Several reasons could account for this: (1) MF % may be more closely correlated with mid-summer (July) peak warmth on the ice cap than with regional mean JJA temperatures; (2) as described earlier, part or the meltwater formed by surface melt in 2003–2006 may have percolated and refrozen in firn from earlier years (early 2000s); and (3) the apparent reversal in the MF trend for 2003–2006 may be simply due to uneven spatial distribution of infiltration ice layers at the coring site (on this subject, see also Appendix B).

[16] For the entire period 1948–2010 ($N = 63$ years), the zero-lag correlation coefficient between 5-year running means of the MF % and regional summer temperature anomalies is $R = 0.55$, taking into account serial autocorrelation and the reduced degrees of freedom [Ebisuzaki, 1997; Santer *et al.*, 2000]. The correlation is significant at the 95% confidence level, and the R value compares well with those previously obtained by Holdsworth [1984] ($0.55 < R < 0.56$). The correlation between MF % and winter temperatures (Figure 2c) is slightly weaker ($R = 0.47$), but also significant. The largest increase in MF %, summer and winter temperatures occurred after the late 1980s, which is consistent with trends in regional and pan-Arctic temperatures [Przybylak, 2007; Graversen *et al.*, 2008], and in glacier mass loss rates in the CAA [Gardner *et al.*, 2011; Sharp *et al.*, 2011]. The mean annual rate of MF increase since 1979 (when the rising trend began), calculated from ice-core data, is $1.02\% \text{ a}^{-1}$ (Table 1). However, when serial autocorrelation and the time-averaging effect of percolation on the MF series are accounted for, the trend is not significant at the 95% level. This underscores the need to average

MF series over longer time intervals to quantify trends in a statistically robust manner (see section 4.2 below). Over the same period 1979–2010, the summer and winter air temperature trends in the eastern Canadian Arctic were 0.05 and $0.08^{\circ}\text{C a}^{-1}$, respectively, and these trends are significant at the 95% level. The rise in MF recorded in the Penny Ice Cap cores is therefore consistent with regional air temperature trends. As equation (1) shows, however, MF % are not determined solely by temperature (melt), but also by the ice accumulation rate. Using selected records from Baffin Island weather stations, Abdalati *et al.* [2004] inferred a slight increase (15%) in precipitation for the Baffin Island region during the 1990s, but regionally-averaged precipitation anomalies for the eastern Arctic (Figure 2d) show little evidence of this. Over the period 1979–2010, the linear trend in precipitation was in fact negative (-0.62 mm a^{-1} ; Table 1). If precipitation did recently increase in the southern Baffin Island region as suggested by Abdalati *et al.* [2004], and if this resulted in higher net ice accumulation on Penny Ice Cap, then the summer melt rates for the corresponding period may be underestimated by the measured MF percentages.

[17] The ice-core record of the past 65 years (Figure 2a) shows that summer melt rates over the past decade at Penny Ice Cap summit were probably the highest since the mid-20th century. The most recent previous episode of comparably high melt rates was in the 1940s and/or early 1950s. This is corroborated by comparing the stratigraphy of firn cores drilled in the summit region of Penny ice cap in 1953, 1979, 1995, 2010 and 2011 (Figure 3). The thick MF sequences that formed during high melt periods in the 1940s to early 1950s, and since the late 1980s, are comparable. The cores taken in 1979 and 1995 show comparatively fewer and thinner MF. As pointed out by Holdsworth [1984], such comparisons must be interpreted with caution because of possible subjective differences in interpretation by different observers. However the reported density values of the “ice” layers observed in 1953 (mean = 720 kg m^{-3} [Ward, 1954]) are comparable to those of MF recorded in the firn stratigraphy in 1995 and 2010–11 (mean = $780 \pm 95 \text{ kg m}^{-3}$), which suggests that these are indeed the same type of features.

3.3. Trends in Firn Temperature

[18] Firn temperatures on Penny Ice Cap summit were recorded at various depths using a thermistor string over the period 1992–2000, and again in 2011. The data from 1992–2000 (Figure 4) show the mean firn temperature at 7.5 m to be $2\text{--}4^{\circ}\text{C}$ warmer than the estimated MAT, which is consistent with findings by Holdsworth [1984] from borehole temperature measurements in 1979. In Figure 5 we compare the firn temperature profiles measured in the summit region of Penny Ice Cap between 1992 and 2000 to the measurements made in 2011. We also show borehole temperature data from 1953 (site A1 in Figure 1) [Ward, 1954] and 1979 (site P79) [Holdsworth, 1984]. The comparison reveals that during most of this 58-year period, the firn temperature at ~ 10 m depth remained relatively constant near -13°C . In contrast, firn temperatures measured in the spring and summer of 2011 show a warming of the firn of nearly 10°C compared to previous decades. While the near-surface readings (<3 m) changed between May and July 2011,

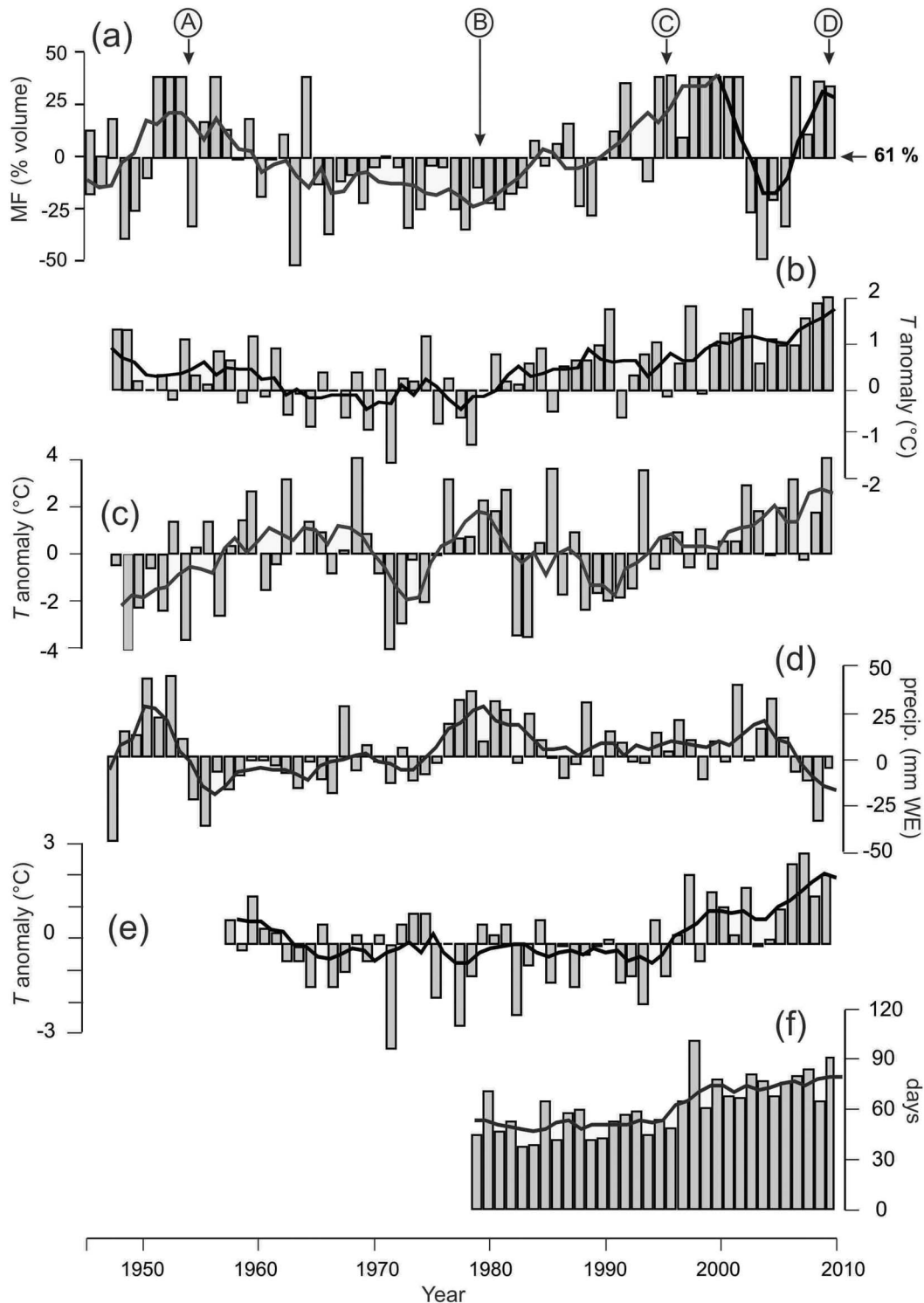


Figure 2. (a) Melt feature (MF) anomalies at the summit of Penny Ice Cap over the period 1945–2010, inferred from firn and ice cores. Circled letters refer to Figure 3. (b) Summer (JJA) and (c) winter (DJF) surface air temperature anomalies in the eastern Canadian Arctic from 1948 to 2010, computed from historical weather station data. (d) Annual precipitation anomalies over the same period [same source]. The period of reference for anomalies shown in Figures 2a–2d is 1961–1990. (e) Summertime (JJA) air temperature anomalies at the 700 hPa level over Penny Ice Cap calculated from NCEP and ERA40 reanalysis model outputs, over the period 1958–2010. (f) Melt season duration at Penny Ice Cap summit, estimated from satellite passive microwave brightness temperature observations over the period 1979–2010. In Figures 2a–2f, a 5-year running mean (bold line) is superimposed on the annual data series.

Table 1. Linear Regression Trends Over the Period 1979–2010 for the Data Series Shown in Figure 2^a

Data Series	<i>N</i>	<i>N_e</i>	Trend	Units
Penny Ice Cap melt features (volume)	32	12	1.02 (0.86)	% a ⁻¹
Eastern Arctic summer surface air temperature	32	25	0.05 (0.01)	°C a ⁻¹
Eastern Arctic winter surface air temperature	32	27	0.08 (0.04)	°C a ⁻¹
Eastern Arctic annual precipitation	32	31	-0.62 (0.31)	mm a ⁻¹
Penny Ice Cap 700 hPa summer air temperature	32	31	0.07 (0.02)	°C a ⁻¹
Penny Ice Cap summit melt season duration	32	29	1.18 (0.24)	days a ⁻¹

^aThe term *N* is the number of observations (years), while *N_e* is the effective sample size, taking into account autocorrelation in the time series. Numbers in parentheses give the standard error on the estimated trends. Bold figures are statistically significant at the 95% level.

reflecting springtime warming, the firn temperatures converge at depth towards -3°C. The 1992–2000 and 2011 measurements were made with the same thermistor types, which rules out major instrumental differences. The firn temperature was also measured independently in July 2011 in a narrow borehole (~0.05 m diameter) using a submersible datalogger (model TR-1050, R. Branker Research Ltd., Ottawa, Ontario). Two recordings at 4.5 and 8.5 m depths gave temperatures of -5 and -0.8°C. The datalogger's temperature readings were later found to deviate slightly from those of a calibrated thermometer, with a possible error of ±1°C. Within these error bounds, however, the datalogger recordings are consistent with those obtained from the thermistors (Figure 5).

[19] The release of latent heat associated with refreezing of percolating meltwater can raise firn temperatures considerably. This has been reported in the Canadian High Arctic [Paterson and Clarke, 1978], in Svalbard [Van De Wal et al., 2002], and on the Greenland Ice Sheet [Pfeffer and Humphrey, 1998]. Holdsworth [1984] used a simple heat transfer model to estimate the magnitude of firn warming (*T'*) at Penny Ice Cap summit due to meltwater refreezing. His model uses a one-dimensional heat flow equation across a semi-infinite solid corresponding to the snowpack, and assumes that all heat is generated at the snow surface and transferred downwards as latent heat. The derived solution describing the temperature rise *T'* in the snow (or firn) due to heat release by meltwater refreezing is:

$$T' = \frac{(Q_L/4)(\rho_s - \rho_i) \exp(-z^2/4\kappa t)}{\rho_s c \sqrt{4\pi\kappa t}} \quad (2)$$

where ρ_s and ρ_i are the mean densities of snow and ice, respectively, z is the depth at which the latent heat is released, t is the relative age of the snow layer considered (e.g., one year), c is the heat capacity and κ the thermal diffusivity of snow, and Q_L is the latent heat of fusion. In his calculations, Holdsworth [1984] assumed a mean annual summer melt percentage of 25% (mass), based on measurements from a 20-m core covering ~30 years of accumulation (Figure 3). His estimated maximum value of *T'* was 3.9°C, which is consistent with the temperature difference between the 10–12 m firn temperature measured in 1979 (-14.4°C) and the estimated MAT at the time. We

performed the same calculation using Holdsworth's heat transfer model, but with a mean annual summer melt percentage of 60% (mass) instead, based on our estimated mean annual MF content of 72% (volume) in the firn at Penny Ice Cap summit over the past 15 years. The values of c and κ in equation (2) were calculated from the mean temperature *T* through the annual snowpack (-20°C) and from ρ_s , following Cuffey and Paterson [2010, pp. 400–401]. Depending on the values used for ρ_i (which can vary from 850 to 910 kg m⁻³) our calculation yields values for *T'* of 12.1 to 14.5°C. This is the estimated warming effect of meltwater refreezing within the annual snowpack. In summers that experienced 100% surface melt (e.g., early 2000s; Figure 2), the warming would have been greater. However if (as is likely) some of the meltwater produced in summer percolates below the annual layer and into the firn below, part of the latent heat is released there, while another part of the energy also escapes to the atmosphere by heating up air. How much of the warming that is produced by summer melt and refreezing is conserved in the firn depends on the depth of meltwater percolation and the summer-winter surface temperature contrast. A better quantification of the impact of the recent warming on the thermal structure of the firn at Penny Ice Cap would require a thermo-physical model simulation that takes into account the formation of ice layers, which is beyond the scope of the present paper. However the calculation presented above shows that latent transfer associated with rising summer melt and percolation could have produced a warming of the magnitude observed in the firn at Penny Ice Cap summit since the mid-1990s.

3.4. Surface Mass Balance

[20] The annual mass balance of ice caps in the QEI is chiefly controlled by summer melt [Koerner, 2005]. Penny Ice Cap receives higher annual snowfall than High Arctic ice caps, but summer melt rates are also greater and are therefore expected to play a determining role in the annual mass budget. Figure 6 shows the present-day SMB gradient, measured on a ~55-km long transect (Figure 1) on the western side of the ice cap. The two mass balance years presented (2007–08 and 2010–11) are those for which the field data are most complete. Snow accumulation on the transect increases slightly with altitude at a mean rate of 0.012 m snow water equivalent (SWE) per 100 m. Below 1200 m, the late winter snow cover is often thin and uneven due to downslope wind scouring. Surface ablation near the glacier margin (<600 m) was ~2.5 m of ice equivalent in 2007–08, but exceeded 3 m of ice equivalent in 2010–11. From airborne laser altimetry surveys, Abdalati et al. [2004] estimated mean thinning rates (=net surface lowering) of 0.2–0.5 m a⁻¹ on the western margin of Penny Ice Cap between 1995 and 2000. Elsewhere on the ice cap margin, thinning rates exceeded 0.4 m a⁻¹ over the same period. Surface ablation rates decrease upslope, and the present-day equilibrium line altitude (ELA) is thought to be between 1450 and 1700 m (Figure 6). A shallow borehole drilled at 1700 m in May 2011 encountered only superimposed ice down to 6 m depth, indicating that for 2010–11, the firn line (the upper limit of perennial snow) had retreated above this altitude. The equilibrium line is expected to lie at the lower limit of the superimposed ice zone.

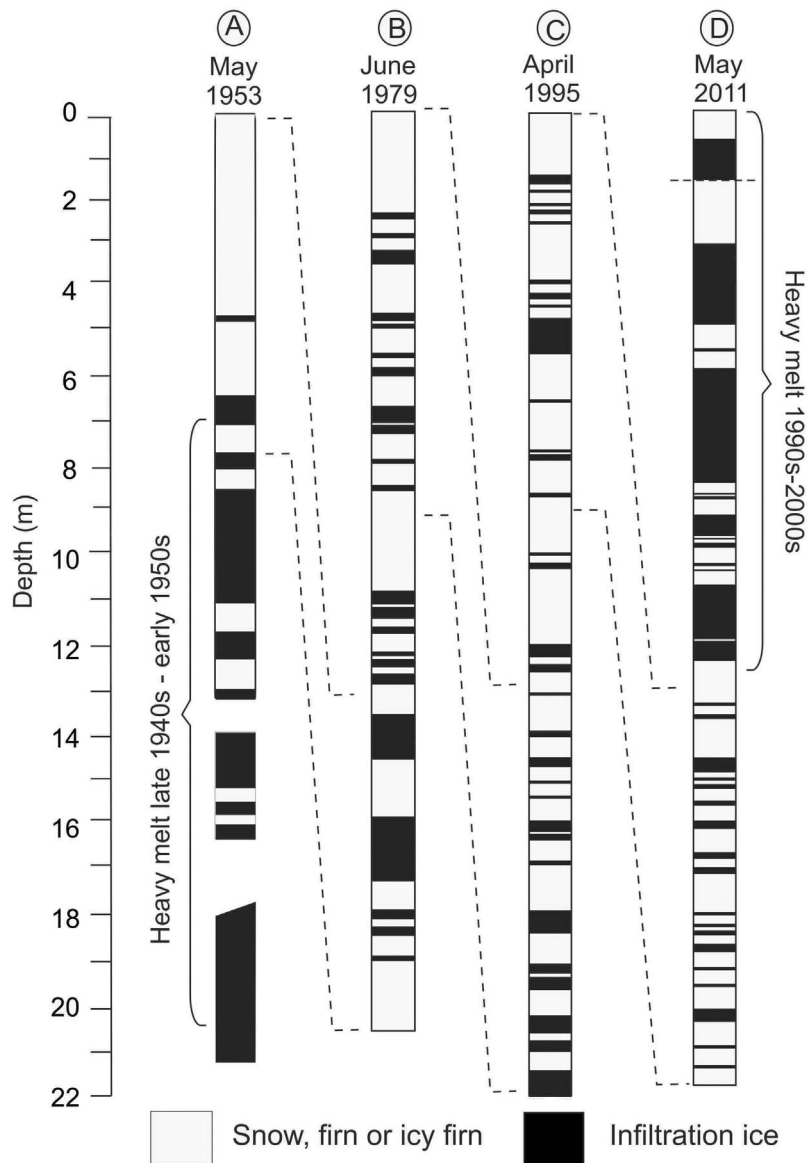


Figure 3. Simplified stratigraphy of firn cores drilled to ~ 20 m depth from the summit region of Penny Ice Cap in 1953 [Ward, 1954], 1979 [Holdsworth, 1984], 1995 (R. Koerner, unpublished data, 1995) and 2010–11 (this work). Infiltration ice layers are shown in black. To minimize interpretive differences between observers, only ice layers thicker than 10 cm are represented. Stippled lines indicate approximate correlative levels.

[21] Recent in situ SMB data for Penny Ice Cap are presently limited to the transect in Figure 6. Future field measurements on other transects will determine how representative this profile is of the ice cap as a whole, and help quantify the current total net mass budget ΔM . Meanwhile, it is instructive to compare the 2007–08 and 2010–11 SMB profiles to measurements made by the 1953 AINA expedition on a different profile facing to the south–southeast, from the highest point on the main ice divide (site A1) to the lower reaches of Highway Glacier (Figure 1) [Orvig, 1954; Ward, 1954]. Altitudes along the 1953 profile were estimated by photogrammetry or theodolite [Orvig, 1954] and may be inaccurate, particularly in the featureless summit area of the ice cap. Thus Weber and Andrieux [1970] give a revised

altitude of 1838 m for site A1, initially reported at 2050 m [Orvig, 1954]. Airborne laser altimetry surveys conducted over Penny Ice Cap since 1995 [Abdalati *et al.*, 2004] suggest an altitude of ~ 1930 m instead. These data indicate that the summit of the ice cap was stable or thickening slightly during 1995–2000. Comparing the 1953, 2007–08 and 2010–11 SMB profiles (Figure 6) shows a reasonable agreement in terms of the ELA. The differences between the 1953 estimate (~ 1380 m) and the 2007–08 and 2010–11 estimates (1450–1700 m) are within the range of observed interannual variability. These figures are also reasonably close to the ELAs measured on other, smaller glaciers in the southeastern Baffin region (~ 900 to 1300 m) [Jacobs *et al.*, 1972; Weaver, 1975; Mokievsky-Zubok *et al.*, 1985].

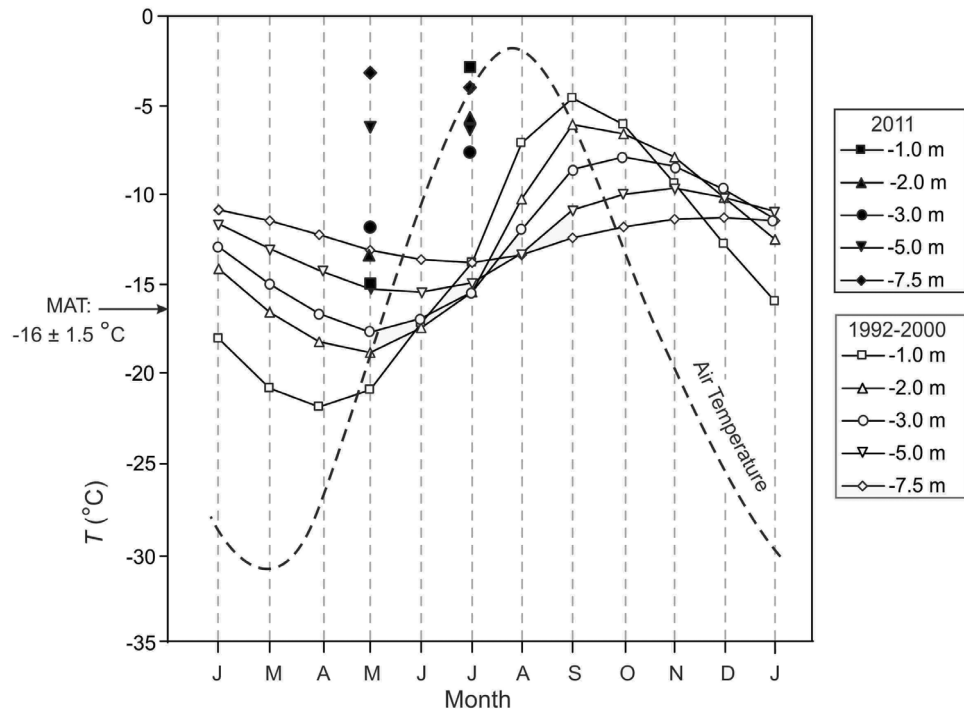


Figure 4. Cycle of mean annual air (~2-m height) and firm temperatures at different depths measured by an automated weather station at the summit of Penny Ice Cap between 1992 and 2000 [Eley, 2001]. Symbols correspond to mean monthly firm temperatures at specific depths, obtained by interpolation of the thermistor data. New thermistor measurements made in May and July 2011 are shown for comparison (shaded symbols).

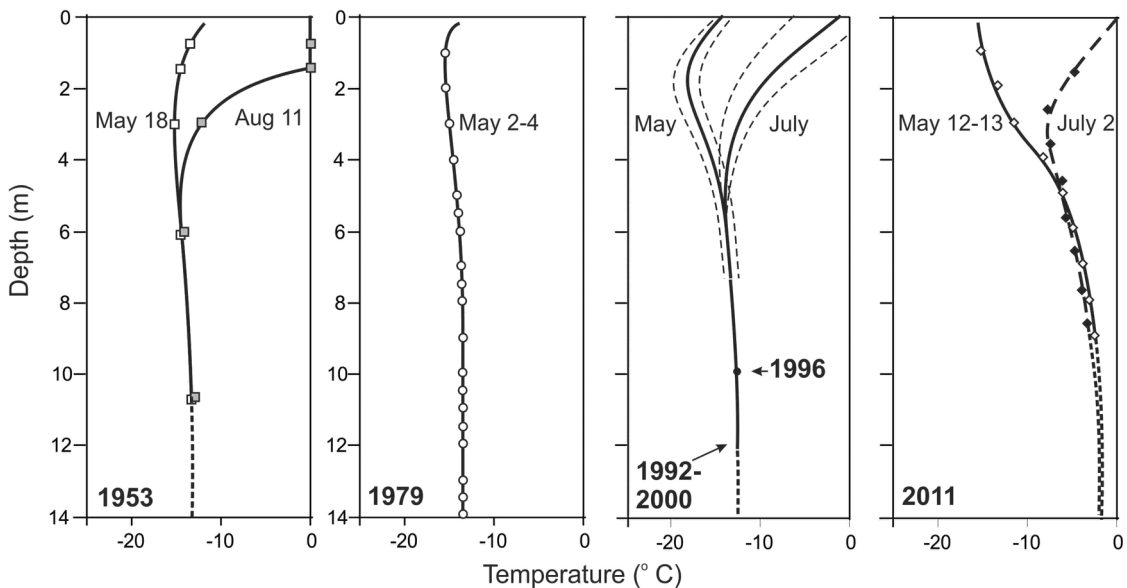


Figure 5. Compared firm temperature profiles to a depth of 14 m in the summit area of Penny Ice Cap measured in the summer of 1953 [Ward, 1954] (site A1 in Figure 1), in May 1979 [Holdsworth, 1984] (site P79), in May and July for 1992–2000 [Eley, 2001] (site AWS) and in May and July of 2011 (this work) (site P95). The 1953 and 1979 measurements extended down to 23 and 20 m, respectively, and temperatures at these depths were the same as at 14 m. The 1953 data are minimum and maximum temperatures over the observation period (May 18–Aug. 11). For the 1992–2000 AWS data, the monthly mean firm temperatures (full lines) and interannual range (stippled lines) in May and July are shown. The point labeled “1996” is the 10-m deep firm temperature measured with a thermistor cable in the P95 borehole in May 1996. Thick stippled line segments on each panel are interpolated or extrapolated from the data.

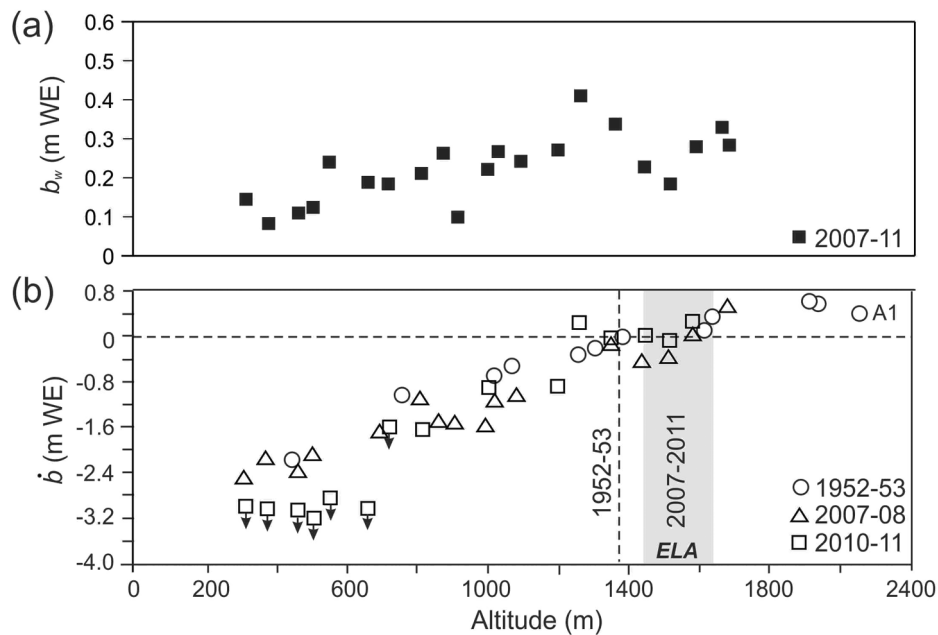


Figure 6. (a) Variations in winter surface mass balance b_w (fall + winter snow accumulation) as a function of altitude, measured on a ~ 55 -km long profile on the southwestern margin of Penny Ice Cap (Figure 1) since 2007. Each point is a median calculated from multiple snowpit observations at the corresponding altitude. (b) Comparison between surface mass balance (b) gradients on two altitudinal profiles across the southern and western sides of Penny Ice Cap (dotted lines in Figure 1), measured in 1953 [Ward, 1954] and between 2007 and 2011 (this work). The vertical stippled line gives the estimated ELA in 1952–53, while the shading gives the estimated range for the ELA over the period 2007–11. Down-pointing arrows indicate that the points shown are minimum estimates for b in the ablation area. Point A1 refers to the summit camp site occupied by members of the 1953 AINA expedition.

3.5. Trends in Snow Densification

[22] Rising summer melt rates on Penny Ice Cap since the late 1980s have led to the formation of numerous thick ice layers in the firn (Figure 3). These have, in turn, increased the densification rate of snow in the uppermost layers of the ice cap's accumulation area. This change is revealed by comparing the firn density profiles measured in the top ~ 20 m of the summit area of Penny Ice Cap using the firn cores drilled in 1953 (site A1; 1930 m), 1995 (site P95; 1860 m) and 2010 (site P2010; 1860 m). The 1995 data come from two parallel cores (85 and 334-m long) drilled one meter apart. While densities were measured in both cores, MF were only recorded in the deeper core. Density measurements were also made on discrete segments of the firn core recovered in 1979 (site P79; ~ 1975 m) (G. Holdsworth, unpublished data, 1979). Density profiles for the different years are compared in Figure 7. A depth of 20 m represents ~ 35 – 40 years of accumulation at the summit of Penny Ice Cap. The 1953 firn densities were measured over large depth increments, which makes detailed comparisons with later years difficult. However, while the 1979 and 1995 firn density profiles are comparable, the 2010 profile shows evidence of a steepening in the density gradient during recent decades, caused by the formation of thick infiltration ice layers. The change in densification rate can be quantified by comparing the cumulative ice-equivalent thicknesses of the 1995 and 2010 firn cores (Figure 7d). At a (true) depth of 20 m, the cumulative ice-equivalent thickness in the

2010 profile is 15.3 m, which is ~ 0.9 m larger than the ice-equivalent thickness at the same depth in the 1995 profile (14.4 m). The extra ice added is mostly accounted for by the thick ice layers formed in the late 1990s and 2000s.

[23] Other, indirect evidence for the impact of high melt rates on snow densification comes from AWS measurements of snow surface settling at the summit of Penny Ice Cap. Full data coverage is only available for the years 1992, 1995, 1996, 2007 and 2010. However, snow surface settling was also monitored at the ice cap summit (site A1) by the AINA summer 1953 expedition [Orvig, 1954]. The 1953 observations only extended through to August 11, but on Orvig's account, the amount of summer melt after that date was probably minimal. These data allow for surface snow settling to be compared for a series of summers of contrasting warmth (Figure 8 and Table 2). The contrast between the coldest seasons (1953, 1992) and some of the warmest ones (2007, 2010) is striking, with snow settling in the latter being nearly an order of magnitude greater than in the former. Changes in snow surface height are the result of surface melt, snow accumulation and wind action (snowdrift). While surface settling on Penny Ice Cap summit appears to start consistently in late June, the timing of renewed net snow accumulation at the end of summer is less regular, varying from late July in 1996 to early September in 2010. As Figure 8 also shows, the length of the melt period (daily air temperatures $>0^\circ\text{C}$), its magnitude (maximum temperatures), and the amount of snow settling are not related in

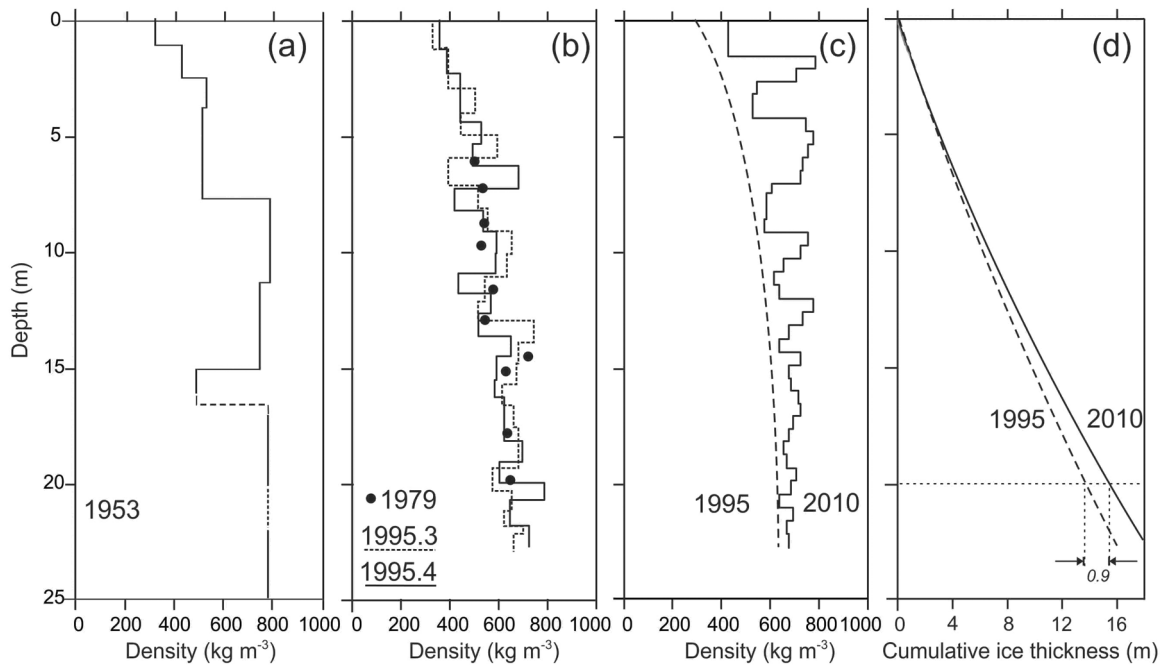


Figure 7. Compared ~ 20 -m firn density profiles at the summit of Penny Ice Cap measured from corings in (a) 1953 [Orvig, 1954; Ward, 1954], (b) 1979 (G. Holdsworth, unpublished data, 1979) and 1995 (R. Koerner, unpublished data, 1995), and (c) 2010 (this work). The 15-m long P95.3 core was drilled one meter away from the 334-m long P95.4 core. Densities in both cores were measured on ~ 1 -m averages, while the 2010 density data are in ~ 55 -cm averages. In Figure 7c, the dashed curve is the smoothed depth-density trend obtained from the 1995 data. (d) Compared cumulative ice-equivalent thicknesses in the 1995 and 2010 firn profiles.

a simple way. Clearly the warmest summers (e.g., 2010) experienced very high surface melt rates, but other warm summers (e.g., 1995) experienced comparatively moderate melt. Possible reasons for these discrepancies are discussed below.

4. Discussion

4.1. Implications of Summer Melt and Firn Temperature Trends

[24] The record of MF developed from Penny Ice Cap cores testifies to an important increase in summer melt rates since the 1980s. On the whole, the data indicate that present-day summer melt rates are probably as great as or greater than they've been at any time in the period of instrumental records from the Canadian Arctic (1948–2010). Comparing the MF record with seasonal temperature anomalies for the eastern Canadian Arctic (Figure 2) shows that both summer and winter air temperatures in this region have risen markedly over the same period. Other signs of recent warming in the southern Baffin region are decreasing sea-ice cover trends over Hudson Bay, Davis Strait and southern Baffin Bay [Moore, 2006; Tivy *et al.*, 2011]. At least some of the decadal sea-ice variability in this region is thought to be driven by the North Atlantic Oscillation [Stern and Heide-Jørgensen, 2003; Kinnard *et al.*, 2006a]. The sea-ice cover decline has been largest since the mid-1990s [Tivy *et al.*, 2011], which is consistent with the observed MF trend in Penny Ice Cap cores. Sea-ice cover reduction may contribute to increased glacier melt rates on southern Baffin Island by

allowing greater oceanic heat fluxes to the atmosphere, particularly in late summer and autumn. The observed regional trends in air temperature and sea ice cover are consistent with the view that increased mass losses on QEI glaciers in the 21st century are driven by anomalously warm sea-surface temperatures in the northwest Atlantic, accompanied by increased southerly warm air advection to the High Arctic in summer via Baffin Bay [Sharp *et al.*, 2011].

[25] An expected consequence of rising summer air temperatures in the eastern Canadian Arctic will be to increase the duration of the summer melt season on glaciers. This has been observed by Dupont *et al.* [2011] on Barnes Ice Cap using spaceborne passive microwave measurements, as described earlier under section 2.6. In Figure 2f, we show the duration of the melt season at Penny Ice Cap summit since 1979, inferred with the same type of measurements and using the same detection algorithm. Based on these data, the length of the melt season has nearly doubled over this period, from 44 days in 1979 to 90 days in 2010. An increase in the duration of the melt season will not necessarily lead, on its own, to a greater volume of MF in the firn, but maintaining surface snow temperatures at 0°C for a greater length of time every summer will facilitate percolation of meltwater in the firn, carrying latent heat with it.

[26] Warming summer temperatures in the eastern Arctic may also have increased the frequency of rainfall events on Penny Ice Cap. This could enhance surface melt rates, as condensation may account for 30% of the surface energy supply at the ice cap summit during the melt season [Orvig, 1954]. Using the European Reanalysis Agency 1 dataset,

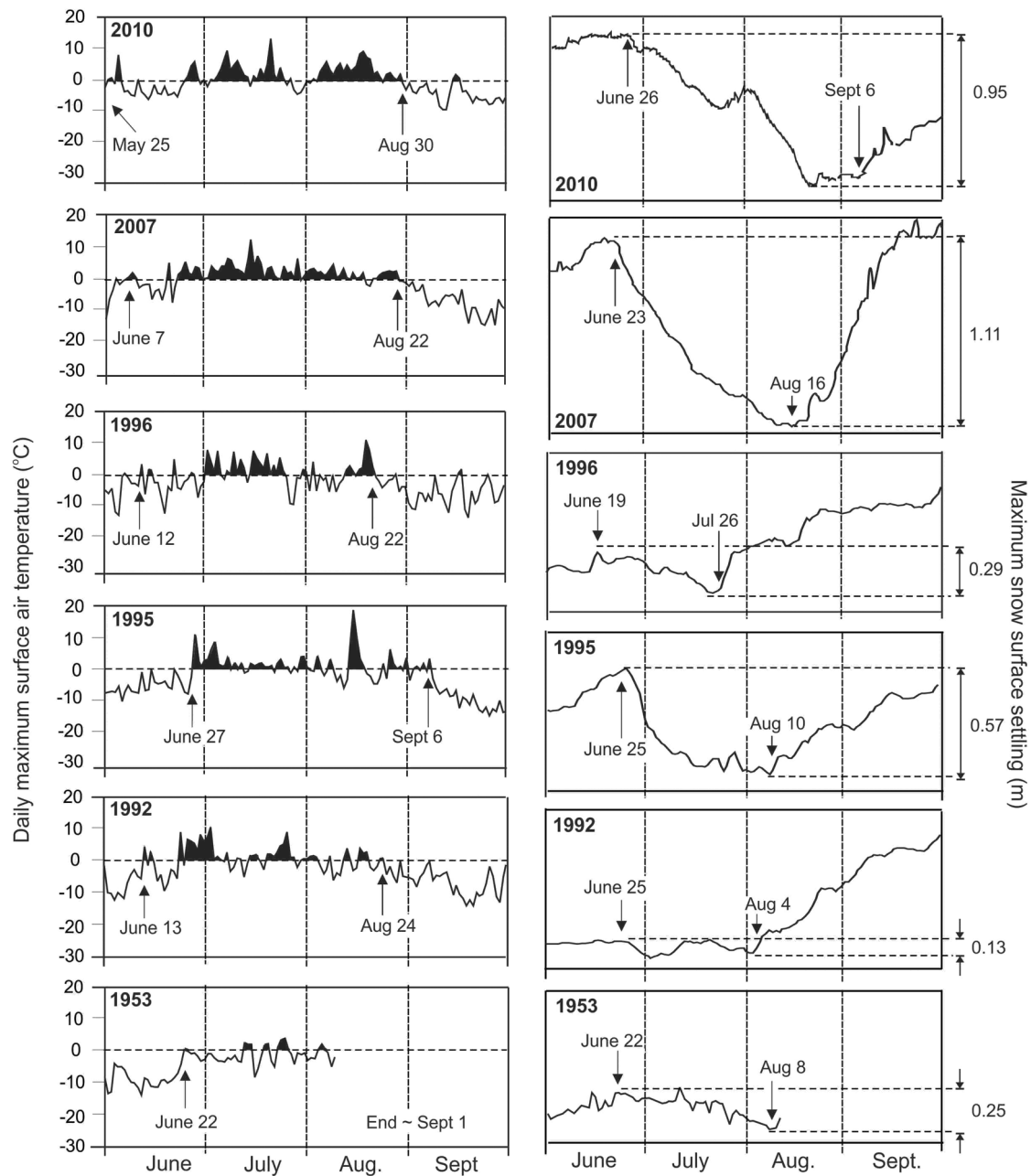


Figure 8. (left) Summer maximum temperatures and (right) snow surface settling in the summit region of Penny Ice Cap in six different years, based on *Orvig* [1954] for the (bottom) summer of 1953 and on ultrasonic depth gauge (UDG) measurements for (top) other years (*Eley* [2001] and this work). Black shading at left denotes days with mean daily surface air temperature $>0^{\circ}\text{C}$. Figures at far right give the estimated maximum vertical settling of the snow surface over the course of the melt season. Dates indicate the approximate onset and close of the melting period (left) and bracket the period of greatest snow settling (right).

Screen and Simmonds [2011] found that rising summer temperatures in the Canadian Arctic since 1989 have been accompanied by a decrease in the snow to total precipitation ratio (SPR), which they ascribe almost entirely to changes in precipitation type (i.e., more frequent rainfall). For the east coast of Baffin Island, the change is most noticeable in late summer (August), with a decrease in SPR of 20 to 30%. Data from southern Baffin Island weather stations (Figure 1)

show that the SPR in this region typically varies between ~ 0.2 and 0.7 in summer (JJA; mean $\pm 1\sigma$) and is usually 1.0 (snowfall only) from October to May. A 20–30% decrease in late summer SPR over this region would translate into a relative decrease in the mean August SPR from 0.5 to ~ 0.6 – 0.7 . At Qikiqtarjuaq, where total precipitation in August averages ~ 40 mm, such an increase would result in additional 1–3 mm of rainfall (on average) relative to the amount

Table 2. Relationship Between Summer Temperatures and Surface Snow Settling Measured at Penny Ice Cap Summit^a

Year	Summer Warmth Ranking	Regional JJA Temperature Anomaly (°C)	Penny Ice Cap Mean JJA Temperature (°C)	Maximum Snow Settling (m)
1953	52	−0.2	−6.1	0.25
1992	56	−0.6	−4.7	0.13
1993	37	0.3	−3.8	—
1994	24	0.7	−5.1	—
1995	15	1.0	−3.5	0.57
1996	50	−0.1	−4.6	0.29
1997	30	0.5	−3.5	—
1998	3	1.8	−1.6	—
1999	48	−0.1	−4.4	—
2007	17	0.9	−1.8	1.11
2008	6	1.5	−1.0	—
2010	1	1.9	−1.7	0.95

^aRegional (eastern Canadian Arctic) summer (JJA) temperature anomalies are computed relative to the 1961–1990 climatological norm, and the ranking of relative summer warmth is for the period 1948–2010 (Environment Canada, online bulletin, 2010). The summer (JJA) surface air temperatures and snow surface settling data for Penny Ice Cap (where available) are from automated weather station recordings. The 1953 data are from *Orvig* [1954]. Italicized figures were estimated from incomplete records (days missing).

of snowfall in that month. The impact of such a small change is unlikely to be very significant at the summit of Penny Ice Cap, compared to the effect of temperature-driven surface melt. However, the effect of rainfall on surface melt rates and MF formation is presently impossible to quantify directly, due to the lack of direct precipitation data from the ice cap.

[27] A remarkable finding of this study is the 10°C warming of firn temperatures (10 m depth) that has occurred at the summit of Penny Ice Cap since the mid-1990s (Figure 5). This finding suggests that the regional warming of the late 1990s and 2000s resulted in a major infusion of latent heat by deep meltwater percolation into the upper firn layers. Interestingly, recent AWS air temperature recordings from the summit of Penny Ice Cap indicate that the MAT over the period 2007–11 has remained close to that measured in the 1990s, i.e. near −16°C. The MAT at the ice cap summit is apparently insensitive to the actual summer warming experienced *in situ*. This may result from the summertime surface radiative energy surplus being largely transferred into the firn by percolation and conduction. Indeed, *Eley* [2001] found that the best predictor for early winter (October to December) firn temperatures at 7.5 m depth on Penny Ice Cap summit was the number of positive degree-days (PDD) in the previous summer. Furthermore to achieve the observed warming of 10°C since the 1990s, much of the latent heat transferred in the firn must be conserved *through* the winter, and this would be facilitated by deep percolation of meltwater [*Van De Wal et al.*, 2002]. Winters in the eastern Canadian Arctic also warmed significantly, albeit irregularly, since the late 1980s (Figure 2), and this may have helped to maintain the present-day “warm” firn temperatures on Penny Ice Cap by reducing the firn-air temperature gradient.

[28] If an increasingly large amount of latent heat is transferred, and retained, into the firn with each successive summer of high melt, this may act as a feedback that

amplifies the summer melt progress on the ice cap forced by regional air temperature trends. In effect, the firn layers are preconditioned by heat storage, such that at the onset of the following melt season, a lesser amount of energy is required to initiate surface melt. This scenario is consistent with the non-linearity between summer melt rates and air temperatures seen in Greenland and on Canadian Arctic ice caps [*Fisher et al.*, 2011]. Some non-linearity is expected even in the absence of an internal feedback, because any large increase in summer mean temperature will lead to a proportionally greater increase in PDD, the amplification being a function of the variance in the temperature cycle [*Reeh*, 1989].

[29] The basal ice temperature under Penny Ice Cap, measured in the P96 borehole (D. Fisher, unpublished data, 1996), was ∼−12°C, slightly warmer than earlier estimates [*Holdsworth*, 1984; *Fisher et al.*, 1998]. If the current rate of internal warming recorded in firn continues uninterrupted, the “warm wave” will gradually propagate through the ice cap by convection and conduction, and the basal ice temperature will eventually rise to the pressure-melting point (PMP). This is expected to alter the drainage of the ice cap and could lead to accelerated velocities of outlet glaciers, as observed in Greenland [e.g., *Zwally et al.*, 2002]. However, spaceborne measurements of ice motion indicate that the velocity of Penny Ice Cap outlets glaciers has actually decreased by 10–20 m a^{−1} since the mid-1980s, which corresponds to an average slowdown of 25% per decade [*Heid and Käbb*, 2011]. Hence, there are, as yet, no indications of dynamical instabilities on Penny Ice Cap such as would be expected if basal temperatures were approaching the PMP.

[30] It is unclear at present if the recent regional warming in the eastern Canadian Arctic extends above an altitude of 2 km. Upper air soundings for southeastern Baffin Island are scarce, making it difficult to seek independent corroborating evidence. As an alternative, we used AWS data, weather station records, and *Orvig*’s [1954] report to compare air temperature lapse rates between Penny Ice Cap summit and the Baffin Bay coast for three different observation periods: summer 1953 (July only), 1992–2000 and 2007–2011 (Figure 9). Presently, the lapse rate is largest in October (∼0.75°C 100 m^{−1}), and decreases through the winter to reach a minimum in February (∼0.15°C 100 m^{−1}) when air temperatures are uniformly cold, or nearly so, from sea level to the summit of the ice cap. At the height of the summer melt period in July, the lapse rate is ∼0.50°C 100 m^{−1}. We found that lapse rates in these months were not noticeably different for the three periods of observations considered (Figure 9). This suggests that the recent warming was felt uniformly over the ∼2000 m altitude range of Penny Ice Cap.

[31] Supportive evidence may be found by examining summertime (JJA) air temperature anomalies at the 700 hPa level over Penny Ice Cap, calculated using overlapping datasets produced by the U.S. National Centers for Environmental Prediction (NCEP) and the European Reanalysis Agency (ERA40) reanalysis models over the period 1958–2010 (Figure 2) (data by A. Gardner, University of Michigan, 2011). The barometric pressure at Penny Ice Cap summit is ∼775 hPa [*Orvig*, 1954], hence temperatures anomalies at 700 hPa provide a good approximation of conditions at this altitude. As Figure 2 shows, the inferred trend and

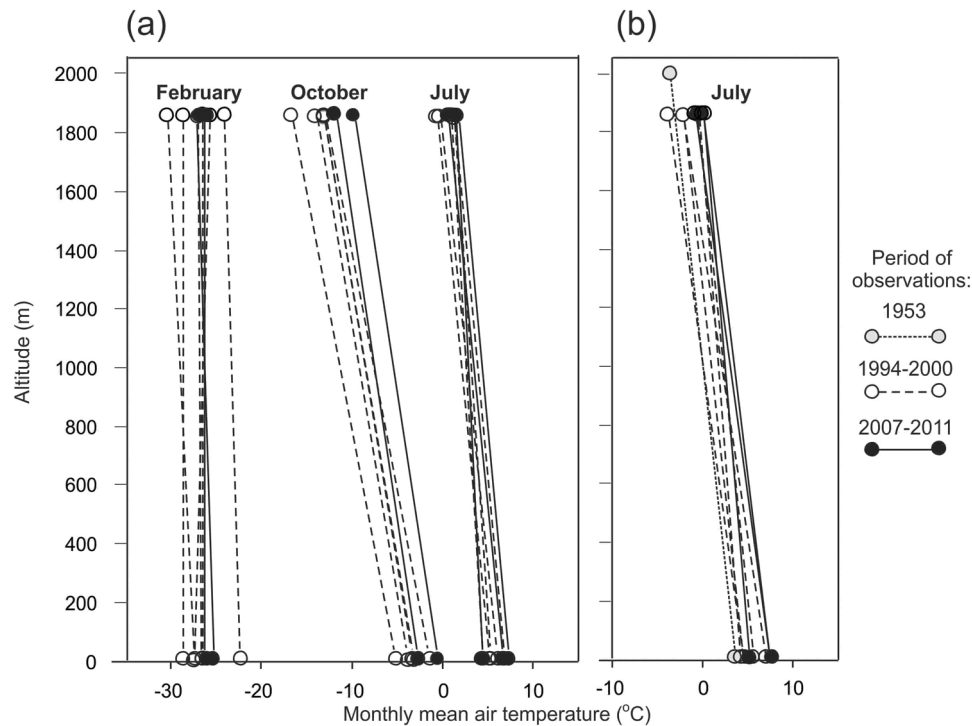


Figure 9. Mean temperature lapse rates compared for selected months between the summit of Penny ice cap and two coastal weather stations, (a) Qikiqtarjuaq and (b) Cape Dyer on southeastern Baffin Island (see Figure 1). The lapse rates in Figure 9a were computed using data from automatic weather stations on Penny Ice Cap (periods 1994–2000 and 2007–11; *Eley* [2001] and this work), and from archived weather station data (Environment Canada, online bulletin, 2010). The lapse rates in Figure 9b also include air temperature recordings made at Penny Ice Cap summit during the 1953 AINA expedition [*Orvig*, 1954]. The period of overlapping data for 1953 is limited to July.

magnitude of JJA air temperature anomalies at 700 hPa in recent decades are closely comparable to the JJA surface air temperature anomalies for the eastern Canadian Arctic, which supports a relatively uniform warming of the lower troposphere. The linear trend in 700 hPa summer temperatures over the period 1979–2010 is $0.07^{\circ}\text{C a}^{-1}$ which is comparable to the trend in surface JJA air temperatures over this period (Table 1). These findings are consistent with those by *Graversen et al.* [2008], although their conclusions were contested on the grounds of heterogeneities in the observational datasets used [*Grant et al.*, 2008]. We also note that a uniform warming over an altitude range of ~ 2000 m would lead to a greater increase in surface melt rates at the low-altitude margins than at the ice cap summit, and this is supported by both our SBM measurements (Figure 6) and by repeat altimetry measurements [*Abdalati et al.*, 2004; *Schaffer et al.*, 2011].

[32] Our findings of rising melt rates on Penny Ice Cap are consistent with increased ice thinning rates observed there and on neighboring Barnes Ice Cap [*Abdalati et al.*, 2004; *Sneed et al.*, 2008; *Schaffer et al.*, 2011]. While *Sneed et al.* [2008] associated the thinning of Barnes ice Cap to regional warming, *Abdalati et al.* [2004] suggested that it could be due to (unspecified) dynamic factors, rather than greater melt rates. The data presented here make it clear that enhanced surface melting could probably account for much or all of the observed net thinning, at least on Penny Ice Cap. However, some thinning may also result from reduced ice

mass transfer rates to the ice cap margin, as suggested by glacier velocity observations of *Heid et Käüb* [2011]. The enhanced densification of the firn due to infiltration ice layer formation (Figure 7) on Penny Ice Cap will need to be accounted for in future attempts to infer ice-cap volume or mass changes using airborne or spaceborne altimetry data [e.g., *Schaffer et al.*, 2011], as it implies an increase in internal mass accumulation. This effect will be quantified in future research.

4.2. The Holocene Record of Summer Melt on Penny Ice Cap

[33] The deep ice cores recovered in 1995–96 from Penny Ice Cap allow us to put recent melt trends, described in earlier sections, in the context of past millennia. Some features of the P95 MF record were presented by *Grumet et al.* [2001], while *Fisher et al.* [2011] offer a comparative analysis of ice-core MF records from several Canadian Arctic ice caps, including Penny. Here we focus our discussion on the significance of this record for the Holocene climate evolution of the southern Baffin Island region.

[34] Of the two long MF series developed from Penny Ice Cap, only that from the P96 core extends beyond 2 ka b.p. [*Okuyama et al.*, 2003]. Figure 10a presents the P96 and composite (P95 and P2010–11) MF records, averaged over 100-year intervals. Owing to wind scouring, the ice accumulation rate at the P96 site is much lower (0.19 m a^{-1}) than at the P95 site (0.37 m a^{-1}), which results in much higher

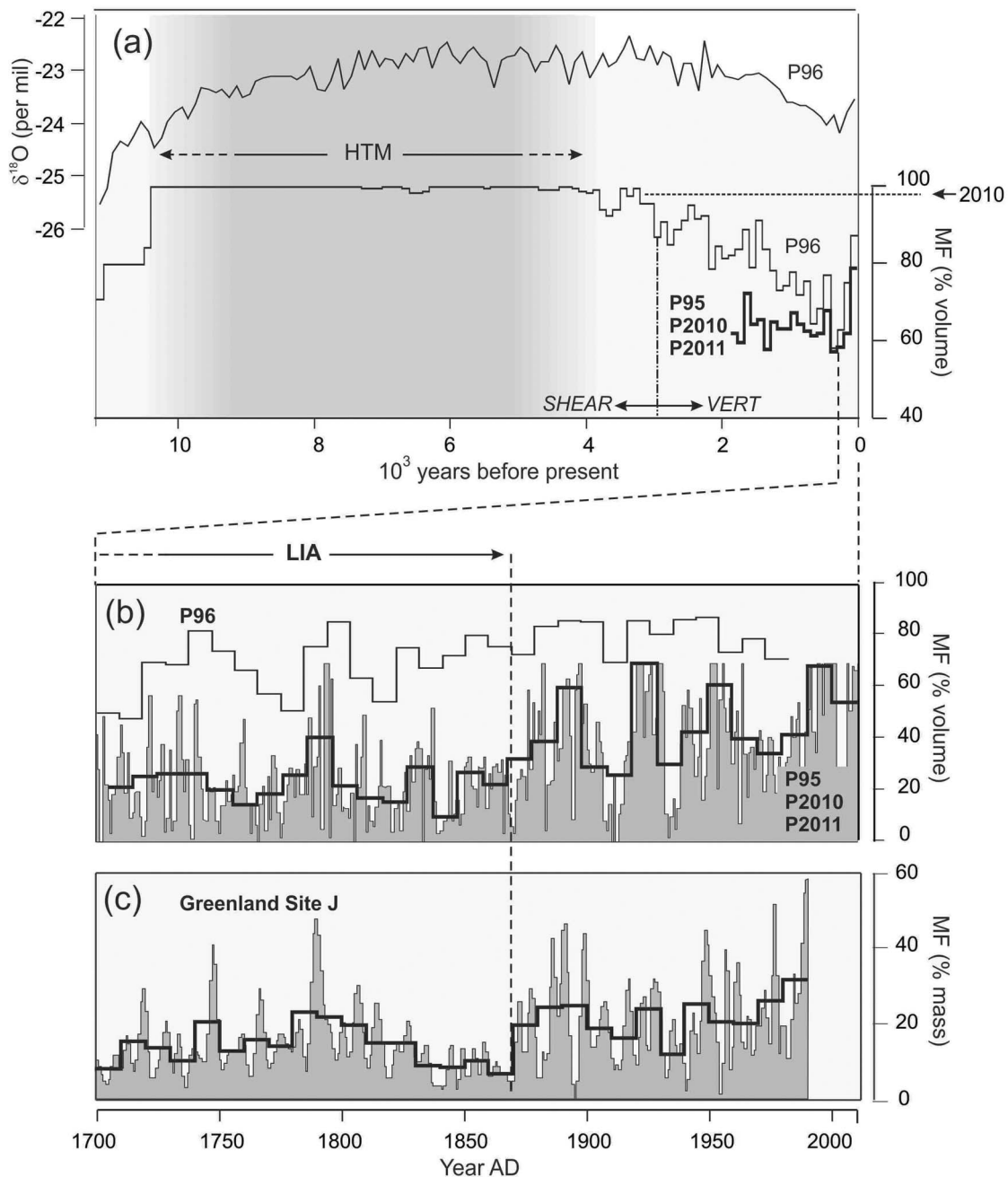


Figure 10. (a) Time series of $\delta^{18}\text{O}$ (100-yr running mean) and melt % from the Penny Ice Cap P96 core [Fisher *et al.*, 1998; Okuyama *et al.*, 2003], compared with the extended melt feature percentage (MF %) record from the P95 coring site (MF in 100-year averages). Shading identifies the early Holocene Thermal Maximum [HTM]. Horizontal stippled line shows the MF % at the P95 coring site in the summer of 2010. Vertical stippled line identifies the inferred transition point between shear-dominated ice flow (SHEAR) and uniaxial vertical compression (VERT) regime in the P96 core [Okuyama *et al.*, 2003]. (b) The past 300 years of melt % in the P96 and the composite P95/P2010–11 records, shown in annual averages (shaded) and 5-year averages (bold). The Little Ice Age cold interval (stippled line) in the southern Baffin Island region came to an end toward the late 19th century [Miller *et al.*, 2005]. (c) The record of MF over the period AD 1700–1989 developed from two ice cores drilled at site J, southern Greenland [Kameda *et al.*, 1995]. As in Figure 10b, the data are shown in 1-year (shaded) and 5-year averages (bold).

MF percentages, from 80 to >90% over the past century [Fisher *et al.*, 1998; Okuyama *et al.*, 2003]. The P96 record shows that for much of the early to mid-Holocene, between ~10 and 4 ka b.p., the coring site experienced 100% melt,

which implies possible discontinuities in the record if the summit of Penny Ice Cap experienced an overall negative mass balance (net wastage and runoff) at any time during this interval. The lack of a trend in the P96 MF during this

period does not imply that regional temperatures were stable, but simply that surface melt rates at this site had reached a maximum (100%). As the $\delta^{18}\text{O}$ record from the P96 core shows (Figure 10a), local temperatures rose to reach a maximum near 6 ka b.p., which is consistent with timing estimates for the Early Holocene Thermal Maximum (HTM) in this region obtained from syntheses of proxy data [Kaufman *et al.*, 2009].

[35] Thereafter, from ~ 4 to 0.5 ka b.p., annual summer melt rates at the P95 and P96 sites declined, following the late Holocene climatic deterioration recorded by numerous proxies across the Arctic [Kaufman *et al.*, 2009], and seen in the P96 $\delta^{18}\text{O}$ profile. The decreasing MF trend in the late Holocene is steeper in the P96 than in the P95 record, and this difference is likely due to the decreasing altitude and accumulation at the P96 site (relative to P95) that resulted from topographic changes on Penny Ice Cap after it separated from the receding Laurentide Ice Sheet. On geological evidence, this separation is thought to have occurred gradually between 8 and 4.5 ^{14}C ka BP (A. Dyke, personal communication, 2011). Isostatic rebound following deglaciation [Kaplan and Miller, 2003] would have affected the P95 and P96 sites nearly equally and can not account for the difference in the MF % trends. The onset of Neoglaciation on Cumberland Peninsula is tentatively dated between 5 and 3 ka b.p. [Miller *et al.*, 2010]. Okuyama *et al.* [2003] measured ice fabric changes in the P96 core that suggests the establishment of the current accumulation regime at this site near the end of the period of very heavy melting ($\sim 100\%$), ~ 3 to 2 ka b.p.

[36] The two Penny Ice Cap MF records of the past 300 years (Figure 10b) both indicate that the late Holocene cooling trend that accompanied Neoglaciation came to an end in the latter half of the 19th century, coincident with the termination of the Little Ice Age (LIA). Since then, summer melt rates have risen steadily, but not monotonically, by ~ 50 – 55% at the summit of the ice cap, with considerable interdecadal variability. The warming since the LIA was punctuated by decadal-scale variability, as attested, for example, by the cooler decades of the 1960s and 70s [Bradley, 1973; Jacobs and Newell, 1979]. The P96 MF record shows decadal variations of lesser amplitude than the P95 record, particularly after AD 1850. This is unsurprising, given that the P96 site, with its lower ice accumulation rate (0.19 m a^{-1}), experiences summer melt rates close to 100%. As a result, MF variations recorded at this site are expected to be less sensitive to regional summer temperature fluctuations than those recorded at the P95 site.

[37] The last ~ 300 years of the Penny Ice Cap summit (P95) MF record show remarkably good agreement with the MF % series developed by Kameda *et al.* [1995] from two cores drilled in southern Greenland (Figure 10c) at a comparable latitude and altitude (Site J; 66°N ; 2030 m). The good correspondence between these records argues for a coherence in the decadal to centennial temperature trends across the southern Baffin Island and southern Greenland region. Extrapolating MF observations (section 3.2.) using the Penny Ice Cap ice-core record indicates that recent melt rates on this ice cap are probably as high now as they have been since the mid-Holocene, ~ 4 to 3 ka b.p. Using contemporary MAT and temperature lapse rates from Penny Ice Cap, we infer that the regional mean July temperature at sea

level during the mid-Holocene may have been as warm as $\sim 8^\circ\text{C}$, i.e. $\sim 4^\circ\text{C}$ warmer than 20th century averages for coastal weather stations along eastern Baffin Island [Miller *et al.*, 2005].

5. Conclusions

[38] In the absence of long-term (>50 year) instrumental climate records for the Baffin Island region, cores recovered from Penny Ice Cap provide a temporal frame of reference in which historical and recent glaciological observations can be placed and synthesized. The story that emerges is consistent. Over the past three decades, Penny Ice Cap, the southernmost major land ice mass on Baffin, entered a phase of particularly intense summer melt and thinning. This was accompanied by a pronounced warming of the upper firn layers which we attribute to latent heat transfer by meltwater percolation. The ice-core MF record shows that Penny Ice Cap experienced comparable, albeit somewhat shorter, previous episodes of high melt rates in the past ~ 150 years, the most recent being in the late 1940s and early 1950s. The present-day (post-1980) intensification of melt on Penny Ice Cap is associated with increasingly positive summer and winter air temperature anomalies in the eastern Arctic, which exceed those of the late 1940s and early 1950s. Rising winter temperatures, in particular, may have contributed to maintain the warmer firn temperatures, thereby preconditioning the ice cap for more intense melt in the subsequent summers. If the present warming trend persists, it is expected that within a few decades, the ice cap will no longer accumulate as firn, but only as superimposed ice, as does Barnes Ice Cap. The present situation on Penny may be a near-future analog for large parts of the nearby (western) Greenland Ice Sheet, which have also experienced increasing summer melt rates in recent decades [Mernild *et al.*, 2011].

[39] When viewed in the longer perspective of the ice-core record, the recent decades of intensified summer melt on Penny Ice Cap follow on a warming trend that began ~ 150 years ago at the close of the LIA, reversing the millennial cooling that characterized the late Holocene climate across the Arctic [Kaufman *et al.*, 2009]. Since the early 1990s, annual summer melt rates at the summit of Penny Ice Cap have risen steadily, such that in recent years, 70 to 100% of annual accumulation was in the form of infiltration ice. The ice-core record indicates that as a result of this warming, the ice cap is now back to a thermal and mass balance state the like of which has probably not been experienced since mid- to early Holocene time, more than 3000 years ago.

Appendix A: Updating the Penny Ice Cap MF Record to 2011

[40] The MF record developed from the P95 deep core ended in the year 1992. In order to update it to the present, a 23-m firn core (P2010) was hand-drilled in May 2010 from the same location, as estimated using a Global Positioning System (GPS) receiver with ~ 10 -m horizontal accuracy. The core was returned frozen to a laboratory in Ottawa, where it was photographed and logged on a light table inside a cold room. Density measurements were performed using

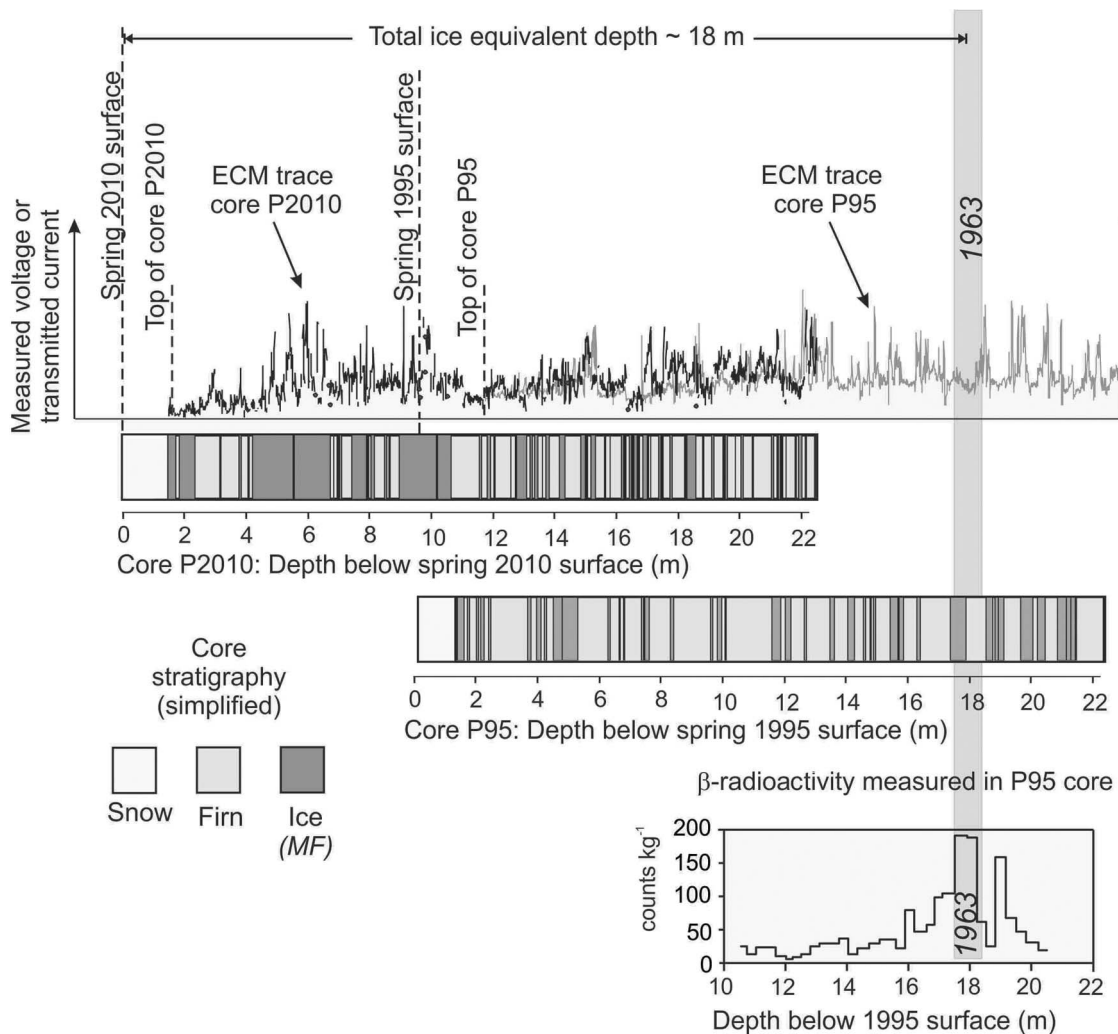


Figure A1. Correlation of core P2010 with core P95 based on stratigraphic features (infiltration ice layers) and ECM trace. The vertical scale on the ECM traces is arbitrary, as the measurements were performed on different instruments with different settings. The 1963 β -activity peak in the P95 core (inset) provides a definitive reference horizon.

calipers and an electronic balance (precision ± 0.005 kg) on over 50 discrete core segments. The solid electrical conductivity of the P2010 core was also measured using a custom-built ECM system. A potential of 1250 V was applied using two brass electrodes with a spacing of 2 cm, and a resistivity bridge of 200 k Ω . In May 2011, a shorter core (P2011; 5.5 m) was also recovered from Penny Ice Cap at a site a few km distant from the P2010 borehole. Its stratigraphy and density were logged in the field.

[41] Visual correlation of the P95 and P2010 cores was based primarily on MF. The thick sequence of infiltration ice layers observed 2 to 11 m down in the P2010 core has no equivalent in the uppermost section of the P95 core, and is therefore inferred to have been formed after the mid-1990s, which is consistent with regional air temperature trends [Przybylak, 2007]. Accordingly, the base of the thick ice layer sequence in the P2010 core was correlated with the top of the P5.4 core (Figure A1). Because meltwater can percolate several meters down in the firn before refreezing, the proposed correlation can only be approximate (± 3 years).

Baseline variations in the ECM trace (transmitted current) of the P2010B core were also compared with those measured in the P95 core. The best visual fit between the overlapping ECM traces was obtained with the end-point of the P95 trace positioned at an ice-equivalent depth of ~ 6.6 m in the P2010 record (Figure A1), which agrees closely with the correspondence inferred from stratigraphic features. Based on this correlation, the mean ice accumulation rate (\bar{A}) for the period 1963–2010, calculated relative to the β -activity peak in the P95 core, is 0.39 m a $^{-1}$. Previous best estimates of \bar{A} varied between 0.36 and 0.39 m a $^{-1}$ [Grumet *et al.*, 1998; Fisher *et al.*, 1998]. Unless precipitation increased or decreased significantly in the Baffin region in the past ~ 20 years, the value of \bar{A} obtained by correlating the P95 and P2010 cores is therefore consistent with previous estimates. In this paper, we used a value of $\bar{A} = 0.37 \pm 0.5$ m a $^{-1}$, based on the best-constrained figure for recent decades [Grumet *et al.*, 1998]. Using this value, the expected time span of the P2010 firn core is ~ 45 years. The short 5.5-m core obtained in May 2011 on Penny Ice Cap was used to estimate the MF

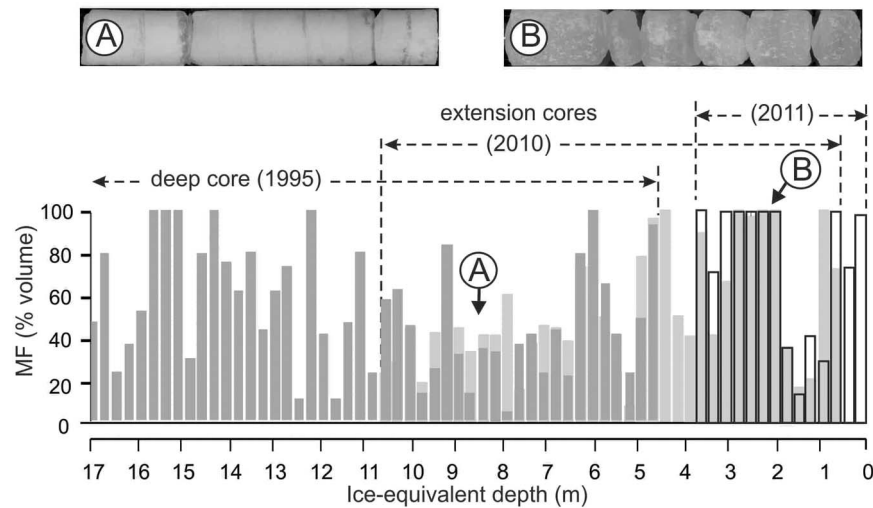


Figure A2. Melt feature (MF) percentages measured in three ice and firn cores from Penny Ice Cap summit (P95, P2010, P2011), overlain to illustrate their correlation: Dark shading = P95 deep core; pale shading = P2010 23-m firn core; outlined = P2011 5.5-m firn core. The data are shown in 0.38 m averages of ice equivalent, which correspond to \sim one-year mean values. Averaged MF percentages of the three cores (combined) are shown in Figure 2 of this manuscript. Insets (A and B) show 0.55-m firn core segments with contrasting infiltration ice content (dark layers). (left) Core A has an estimated volumetric MF content of \sim 20% (including interstitial ice in the firn), whereas (right) core B is 100% infiltration ice.

percentage for the balance year 2010–11. Melt feature % estimates for 2009–2010 in the 2011 firn core were consistent with those of the P2010 core for the same years. The final, updated MF record for Penny Ice Cap summit (Figure 2) was obtained by averaging the MF % of overlapping parts in the P95, P2010 and P2011 cores (Figure A2).

Appendix B: Error Estimates for the Penny Ice Cap MF Record

[42] The principal sources of uncertainty in the ice-core MF series shown in Figures 2 and 10 are (1) errors in the depth-age model, and (2) the spatial variability of MF (the “stratigraphic noise” [Fisher *et al.*, 1985]). Dating errors are somewhat dependent on the MF variability in ice cores, because changes in annual ice accumulation rates will affect the depth-age scale and the corresponding time-averaged MF percentages.

B1. Dating Errors

[43] The depth-age models for the Holocene segments of the P95 and P96 cores developed by Fisher *et al.* [1998] are constrained by reference horizons which include spikes in the electrical conductivity (ECM) and sulphate (SO_4^{2-}) profiles of the cores ascribed to acidic fallout of known historical eruptions previously identified in central Greenland cores. The most unequivocal is the Laki eruption (Iceland, AD 1783). Another reference horizon is the 1962–63 spike in β -radioactivity detected at a depth of 18 m in the P95 core (data by C. Wake and J. Dibb, University of New Hampshire, 1995). The Holocene-Wisconsin transition was assigned an age of 11,550 years before present (b.p.) based on the midpoint of the $\delta^{18}\text{O}$ step at the Younger Dryas - Preboreal boundary, as dated in the GISP2 and GRIP Greenland cores

[Johnsen *et al.*, 1992; Alley *et al.*, 1997]. This age estimate has since been revised to 11,703 yr b.p. [Rasmussen *et al.*, 2006] but the adjustment has little effect on the depth-age relationship of the Penny Ice Cap cores for most of the Holocene. The depth-age model between the control points was developed by spectral analysis of the ECM signal for the P95 core [Fisher *et al.*, 1998], and by interpolation using a simple ice-flow model [Nye, 1963] in the P96 core.

[44] Table A1 gives the model-predicted age of the ice in the P95 and P96 cores at various reference horizons of known or presumed age. These figures provide estimates of the models’ accuracy at various depths. Owing to the lack of distinct reference horizons, the largest dating uncertainties occur in the mid- to early Holocene (between \sim 8 and 4 ka b.p.). Dating errors in this part of the P95 and P96 records may be as large as \pm 500 years, based on a comparison of different depth-age model iterations [Fisher *et al.*, 1998, Figure 5]. Regardless of intrinsic model errors, departures from predicted ages between control points may also occur if the net annual ice accumulation rate (A) in the corresponding time interval deviates significantly from its long-term mean value \bar{A} . The resulting dating errors will be largest halfway between any pair of time-control points. These errors were estimated using a Monte-Carlo simulation in which A is allowed to vary randomly from year to year with a maximum departure dA relative to \bar{A} [Kinnard *et al.*, 2006b]. For Penny Ice Cap, we used a value of $dA = 25\%$ (relative standard deviation about \bar{A}), which is a realistic, if conservative, figure based on field measurements. For greater realism, the temporal variance of A in the simulation was represented by a blue noise model, following Fisher *et al.* [1985]. Results showed that the maximum error on the estimated age of the ice introduced by variations in A never exceeds \pm 8 years (95% confidence interval), and is typically much less, for any time interval

Table A1. Estimated Dating Errors in the Penny Ice Cap P95 and P96 Deep Cores, Based on a Comparison Between Reference Horizons of Known Age, and Their Age as Predicted by the Depth-Age Model Used^a

Reference Horizon/Event	True Age of Event		Ice-Core Signature	Depth of Reference Horizon in P95 Ice Core		Model Age ^b Years Before 2010	Dating Error	
	Calendar (BC/AD)	Years Before 2010		Real (m)	Ice Equivalent (m)		Years	Relative to True Age (%)
<i>P95 Core (Length = 334 m; Mean Ice Accumulation Rate = 0.38 m a⁻¹)</i>								
Surface nuclear bomb tests	AD 1963	47	β -radioactivity	17.70	11.75	47	0	0.0
Katmai eruption (Alaska)	AD 1912	98	SO ₄ , acidity (ECM)	41.39	33.50	93	5	5.9
Tambora eruption (Indonesia)	AD 1816	194	SO ₄ , acidity (ECM)	76.14	68.03	186	8	4.3
Laki eruption (Iceland)	AD 1783	227	SO ₄ , acidity (ECM)	83.66	75.55	211	16	7.4
Eruption (unknown source)	AD 1259	751	SO ₄ , acidity (ECM)	173.12	164.54	799	48	6.4
Eldja eruption (Iceland)	AD 933	1076	SO ₄ , acidity (ECM)	193.03	184.20	1015	61	5.7
Eruption (unknown source)	50 BC	2060	SO ₄ , acidity (ECM)	256.82	247.15	2092	32	1.6
Wisconsin-Holocene transition ^c		11713	$\delta^{18}\text{O}$	306.72	316.55	11713	0	0
<i>P96 Core (Length = 179 m; Mean Ice Accumulation Rate = 0.19 m a⁻¹)</i>								
Katmai eruption (Alaska)	AD 1912	98	SO ₄ , acidity (ECM)	19.79	17.04	99	1	1.0
Laki eruption (Iceland)	AD 1783	227	SO ₄ , acidity (ECM)	43.08	39.94	227	0	0.0
Eruption (unknown source)	AD 1259	751	SO ₄ , acidity (ECM)	94.26	90.19	752	1	0.1
Eruption (unknown source)	O A.D.	2010	SO ₄ , acidity (ECM)	142.91	137.68	2068	58	2.9
Wisconsin-Holocene transition ^c		11713	$\delta^{18}\text{O}$	169.78	164.25	11713	0	0

^aDating errors are likely to be largest in the early Holocene (between 10,000 and 5000 years before present).

^bModel refers to the latest version of the depth-age scale [Fisher *et al.*, 1998].

^cMid-point of $\delta^{18}\text{O}$ step at the Younger Dryas–Preboreal transition. Revised estimated age as per Greenland GICC05 time scale [Rasmussen *et al.*, 2006].

between age control points (Table A1) in the last ~ 2000 years. Earlier in the record, intrinsic model-related dating errors are comparatively much larger.

B2. Stratigraphic Noise

[45] Melt features in firm are highly variable and often discontinuous over spatial scales of 10^2 – 10^6 m² owing to the heterogeneity of the snowpack structure. This introduces “stratigraphic noise” in the MF time series that obscures the climatic signal related to seasonal temperature variations. In the late Holocene part of the Penny ice-core record, the uncertainty about the “true” value of the MF percentage resulting from stratigraphic noise is likely to be much larger than that introduced by depth-age uncertainties. The amount of stratigraphic noise (spatial variability) in any ice-core variable can be estimated by correlating time series developed from parallel cores separated by a known distance [Fisher *et al.*, 1985; Fisher and Koerner, 1994; Kuhns *et al.*, 1997]. On Devon Ice Cap, D. Fisher (unpublished data, 1977) found that the mean correlation coefficient between 5-year averaged MF series from three parallel cores spaced by a few tens of meters was $\bar{R}_{MF} \approx 0.50$ (length of series = 650 years; mean MF percentage $\approx 6\%$). Using 100-year averages of the MF data, \bar{R}_{MF} increased to 0.60. A similar comparison of two parallel cores drilled on Agassiz Ice Cap gave a value of $\bar{R}_{MF} = 0.45$ for 5-year averaged MF series (length of series = 950 years; mean MF percentage $\approx 4\%$) [Fisher and Koerner, 1994]. At site J, southern Greenland (66°N; 2030 m), Kameda *et al.* [1995] obtained a correlation of 0.80 between 5-year averaged MF series in two cores drilled one meter apart (length of series ≈ 60 years; mean MF percentage $\approx 21\%$).

[46] We do not have multiple MF series from Penny Ice Cap summit, so the spatial variability could not be estimated

directly. The much higher annual surface melt rates on this ice cap, relative to QEI ice caps or southern Greenland, are expected to result in greater spatial coherence between MF, because thicker ice layers are also more horizontally continuous. However in the absence of direct quantitative evidence for this, we adopt conservative estimates of \bar{R}_{MF} equal to 0.4, 0.55 and 0.6, respectively, for 5-, 10- and 100-yr averages of the MF percentages in the late Holocene record from Penny Ice Cap (\sim the last 2000 years). The true value of R_{MF} is likely to vary over time with summer melt rates. From \bar{R}_{MF} , the mean signal-to-noise variance ratio F in the Penny Ice Cap MF time series can be estimated following the formulation of Fisher *et al.* [1985]:

$$F = \frac{\text{var}(S)}{\text{var}(e)} = \frac{\bar{R}_{MF}}{1 - \bar{R}_{MF}}$$

where $\text{var}(S)$ and $\text{var}(e)$ are the variance contributions of the climate signal and the noise (spatial, temporal) in the MF time series, respectively. Using $\bar{R}_{MF} = 0.4$ for 5-year averaged MF series gives $F = 0.67$. For 10-year averages ($\bar{R}_{MF} = 0.55$), we get $F = 1.22$, and for 100-yr averages ($\bar{R}_{MF} = 0.6$), we get $F = 1.5$.

[47] **Acknowledgments.** Mass balance measurements on Penny Ice Cap were conducted with support from the staff at Auyuituq National Park, the community of Pangnirtung and with field assistance by C. Kinnard, S. Akeagok, D. Kilabuk, V. Ter-Emmanuilyan, A. Bevington, P. Peyton and C. Latour. Aircraft support was provided by the Polar Continental Shelf Project. This research was conducted as part of Natural Resources Canada’s Climate Change Geoscience program, with additional funding support from the International Polar Year initiative (Indian and Northern Affairs Canada), Natural Science and Engineering Research Council of Canada, Canada Foundation for Innovation, Ontario Research Fund, and the Northern Scientific Training Program. This is contribution 20110335 from Natural Resources Canada, Earth Science Sector.

References

- Abdalati, W., W. Krabill, E. Frederick, S. Manizade, C. Martin, J. Sonntag, R. Swift, R. Thomas, J. Yungel, and R. Koerner (2004), Elevation changes of ice caps in the Canadian Arctic Archipelago, *J. Geophys. Res.*, *109*, F04007, doi:10.1029/2003JF000045.
- Alley, R. B., et al. (1997), Visual-stratigraphic dating of the GISP2 ice core: Basis, reproducibility and application, *J. Geophys. Res.*, *102*, 26,367–26,381, doi:10.1029/96JC03837.
- Ashcraft, I. S., and D. G. Long (2006), Comparison of methods for melt detection over Greenland using active and passive microwave measurements, *Int. J. Remote Sens.*, *27*, 2469–2488, doi:10.1080/01431160500534465.
- Baird, P. D. (1952), Method of nourishment of the Barnes ice cap, *J. Glaciol.*, *2*, 2–9.
- Baird, P. D. (1953), Baffin Island expedition, 1953: A preliminary field report, *Arctic*, *6*, 227–251.
- Bell, C., D. Mair, D. Burgess, M. Sharp, M. Demuth, F. Cawkwell, R. Bingham, and J. Wadhams (2008), Spatial and temporal variability in the snowpack of a High Arctic ice cap: Implications for mass-change measurements, *Ann. Glaciol.*, *48*, 159–170.
- Blake, W. (1953), Studies of the Grinnell Glacier, Baffin Island, *Arctic*, *6*, p. 167.
- Bradley, R. S. (1973), Seasonal climatic fluctuations on Baffin Island during the period of instrumental records, *Arctic*, *26*, 230–243.
- Cogley, J. G., et al. (2011), *Glossary of Glacier Mass Balance and Related Terms*, *Tech. Doc. Hydrol.*, vol. 86, 114 pp., Int. Assoc. Cryospheric Sci., Paris.
- Cuffey, K. M., and W. S. B. Paterson (2010), *The Physics of Glaciers*, 4th ed., 701 pp., Elsevier, Amsterdam.
- Dupont, F., A. Royer, A. Langlois, A. Gressent, G. Picard, M. Fily, P. Cliche, and M. Chum (2011), Monitoring the melt season length of the Barnes ice cap over the 1979–2010 period using active and passive microwave remote sensing data, paper presented at 68th Conference, East. Snow. Conf., Montreal, Canada, 14–16 June.
- Ebisuzaki, W. (1997), A method to estimate the statistical significance of a correlation when the data are serially correlated, *J. Clim.*, *10*, 2147–2153, doi:10.1175/1520-0442(1997)010<2147:AMTETS>2.0.CO;2.
- Eley, J. (2001), Penny Ice Cap auto weather station 1992–2000: Interannual variations of temperature and snow growth, internal report, 19 pp., Clim. Res. Branch, Meteorol. Ser. Can., Saskatoon, Sask., Canada.
- Fisher, D. A., and R. M. Koerner (1994), Signal and noise in four ice-core records from the Agassiz Ice Cap, Ellesmere Island, Canada: Details of the last millennium for stable isotopes, melt and solid conductivity, *Holocene*, *4*, 113–120, doi:10.1177/095968369400400201.
- Fisher, D. A., N. Reeh, and H. B. Clausen (1985), Stratigraphic noise in time series derived from ice cores, *Ann. Glaciol.*, *7*, 76–86.
- Fisher, D. A., et al. (1998), Penny Ice Cap cores, Baffin Island, Canada, and the Wisconsin Foxe Dome connection: Two states of Hudson Bay ice cover, *Science*, *279*, 692–695, doi:10.1126/science.279.5351.692.
- Fisher, D., J. Zheng, D. Burgess, C. Zdanowicz, C. Kinnard, M. Sharp, and J. Bourgeois (2011), Recent melt rates of Canadian Arctic ice caps are the highest in four millennia, *Global Planet. Change*, *84–85*, 3–7, doi:10.1016/j.gloplacha.2011.06.005.
- Fritzsche, J. (2011), Temperature trends in Canada, *EnviroStats Bull.*, *5*, 2–9.
- Gardner, A. S., G. Moholdt, B. Wouters, G. J. Wolken, D. O. Burgess, M. J. Sharp, G. Cogley, C. Braun, and C. Labine (2011), Sharply increased mass loss from glaciers and ice caps in the Canadian Arctic Archipelago, *Nature*, *473*, 357–360, doi:10.1038/nature10089.
- Goto-Azuma, K., R. M. Koerner, and D. A. Fisher (2002), An ice-core record over the last two centuries from Penny Ice Cap, Baffin Island, Canada, *Ann. Glaciol.*, *35*, 29–35, doi:10.3189/172756402781817284.
- Grant, A. N., S. Brönnimann, and L. Haimberger (2008), Recent Arctic warming vertical structure contested, *Nature*, *455*, 2–3, doi:10.1038/nature07257.
- Graversen, R. G., T. Mauritsen, M. Tjernström, E. Källén, and G. Svensson (2008), Vertical structure of recent Arctic warming, *Nature*, *451*, 53–56, doi:10.1038/nature06502.
- Grumet, N. S., C. P. Wake, G. A. Zielinski, D. Fisher, R. Koerner, and J. D. Jacobs (1998), Preservation of glaciochemical time-series in snow and ice from the Penny Ice Cap, Baffin Island, *Geophys. Res. Lett.*, *25*, 357–360.
- Grumet, N. S., C. P. Wake, P. A. Mayewski, G. A. Zielinski, S. I. Whitlow, R. M. Koerner, D. A. Fisher, and J. M. Woollett (2001), Variability of sea-ice in Baffin Bay over the last millennium, *Clim. Change*, *49*, 129–145, doi:10.1023/A:1010794528219.
- Hammer, C. U. (1980), Acidity of ice cores in relation to absolute dating, past volcanism and radio-echoes, *J. Glaciol.*, *25*, 359–372.
- Heid, T., and A. Kääb (2011), Worldwide widespread decadal-scale decrease of glacier speed revealed using repeat optical satellite images, *Cryosphere Discuss.*, *5*, 3025–3051, doi:10.5194/tcd-5-3025-2011.
- Holdsworth, G. (1984), Glaciological reconnaissance of an ice core drilling site, Penny Ice Cap, Baffin Island, *J. Glaciol.*, *30*, 3–15.
- Jacob, T., J. Wahr, T. Pfeffer, and S. Swenson (2012), Recent contributions of glaciers and ice caps to sea level rise, *Nature*, *482*, 514–518, doi:10.1038/nature10847.
- Jacobs, J. D. (1990), Integration of automated station data into objective mapping of temperatures for an Arctic region, *Climatol. Bull.*, *24*, 84–96.
- Jacobs, J. D., and J. P. Newell (1979), Recent year-to-year variations in seasonal temperatures and sea ice conditions in the eastern Canadian Arctic, *Arctic*, *32*, 345–354.
- Jacobs, J. D., J. T. Andrews, R. G. Barry, R. S. Bradley, R. Weaver, and L. D. Williams (1972), Glaciological and meteorological studies on the Boas Glacier, Baffin Island, for two contrasting seasons (1969–70 and 1970–71), *Int. Assoc. Sci. Hydrol. Publ.*, *107*, 371–382.
- Johnsen, S. J., H. B. Clausen, W. Dansgaard, K. Fuhrer, N. Gundestrup, C. U. Hammer, P. Iversen, J. Jouzel, B. Stauffer, and J. P. Steffensen (1992), Irregular glacial interstadials recorded in a new Greenland ice core, *Nature*, *359*, 311–313, doi:10.1038/359311a0.
- Kameda, T., H. Narita, H. Shoji, F. Nishio, Y. Fujii, and O. Watanabe (1995), Melt features in ice cores from Site J, southern Greenland: Some implications for summer climate since AD 1550, *Ann. Glaciol.*, *21*, 51–58.
- Kaplan, M. R., and G. H. Miller (2003), Early Holocene deleveling and deglaciation of the Cumberland Sound region, Baffin Island, Arctic Canada, *Geol. Soc. Am. Bull.*, *115*, 445–462, doi:10.1130/0016-7606(2003)115<0445:EHDADO>2.0.CO;2.
- Kaufman, D. S., et al. (2009), Recent warming reverses long-term Arctic cooling, *Science*, *325*, 1236–1239, doi:10.1126/science.1173983.
- Kinnard, C., C. Zdanowicz, D. Fisher, B. Alt, and S. McCourt (2006a), Climatic analysis of sea-ice variability in the Canadian Arctic from operational charts, 1980–2004, *Ann. Glaciol.*, *44*, 391–402, doi:10.3189/172756406781811123.
- Kinnard, C., C. Zdanowicz, D. Fisher, and C. Wake (2006b), Calibration of an ice-core glaciochemical (sea salt) record with sea ice variability in the Canadian Arctic, *Ann. Glaciol.*, *44*, 383–390, doi:10.3189/172756406781811349.
- Knowles, K. W., E. G. Njoku, R. L. Armstrong, and M. J. Brodzik (2002), Nimbus-7 SMMR Pathfinder Daily EASE-Grid Brightness Temperatures, <http://nsidc.org/data/nsidc-0071.html>, Natl. Snow and Ice Data Cent., Boulder, Colo.
- Koerner, R. M. (1977), Devon Island ice cap: Core stratigraphy and paleoclimate, *Science*, *196*, 15–18, doi:10.1126/science.196.4285.15.
- Koerner, R. M. (2005), Mass balance of glaciers in the Queen Elizabeth Islands, Nunavut, Canada, *Ann. Glaciol.*, *42*, 417–423, doi:10.3189/172756405781813122.
- Kuhns, H., C. Davidson, J. Dibb, C. Stearns, M. Bergin, and J.-L. Jaffrezo (1997), Spatial and temporal variability of snow accumulation in central Greenland, *J. Geophys. Res.*, *102*, 30,059–30,068, doi:10.1029/97JD02760.
- Maslanik, J., and J. Stroeve (2011), DMSP SSM/I-SSMIS Daily Polar Gridded Brightness Temperatures, <http://nsidc.org/data/nsidc-0001.html>, Natl. Snow and Ice Data Cent., Boulder, Colo.
- Maxwell, J. B. (1981), Climatic regions of the Canadian Arctic Islands, *Arctic*, *34*, 225–240.
- Memild, S. H., T. L. Mote, and G. E. Liston (2011), Greenland ice sheet surface melt extent and trends:1960–2010, *J. Glaciol.*, *57*, 621–628, doi:10.3189/002214311797409712.
- Milewska, E., and W. D. Hogg (2001), Spatial representativeness of a long-term climate network in Canada, *Atmos. Ocean*, *39*, 145–161, doi:10.1080/07055900.2001.9649671.
- Miller, G. H., A. P. Wolfe, J. P. Briner, P. E. Sauer, and A. Nesje (2005), Holocene glaciation and climate evolution of Baffin Island, Arctic Canada, *Quat. Sci. Rev.*, *24*, 1703–1721, doi:10.1016/j.quascirev.2004.06.021.
- Miller, G. H., et al. (2010), Temperature and precipitation history of the Arctic, *Quat. Sci. Rev.*, *29*, 1679–1715.
- Mokievsky-Zubok, O., C. S. L. Ommann, and J. Power (1985), Glacier mass balance 1965–1984 (Cordillera and Arctic), technical report, 59 pp., Natl. Hydro. Res. Inst., Environ. Can., Ottawa.
- Moore, G. W. K. (2006), Reduction in seasonal sea ice concentration surrounding southern Baffin Island, 1979–2004, *Geophys. Res. Lett.*, *33*, L20501, doi:10.1029/2006GL027764.
- Nye, J. F. (1963), Correction factor for accumulation measured by the thickness of the annual layers in an ice sheet, *J. Glaciol.*, *4*, 785–788.
- Okuyama, J., H. Narita, T. Hondoh, and R. M. Koerner (2003), Physical properties of the P96 ice core from Penny Ice Cap, Baffin Island, Canada, and derived climatic records, *J. Geophys. Res.*, *108*(B2), 2090, doi:10.1029/2001JB001707.
- Orvig, S. (1954), Glacial-meteorological observations on ice caps in Baffin Island, *Geogr. Ann.*, *36*, 193–318, doi:10.2307/520205.

- Østrem, G., and M. M. Brugman (1991), Glacier mass-balance measurements: A manual for field and office work, *Tech. Rep. 4*, 224 pp. Natl. Hydrol. Res. Inst., Environ. Can., Saskatoon, Sask., Canada.
- Paterson, W. S. B., and G. K. C. Clarke (1978), Comparison of theoretical and observed temperature profiles in Devon Island ice cap, Canada, *Geophys. J. R. Astron. Soc.*, *55*, 615–632, doi:10.1111/j.1365-246X.1978.tb05931.x.
- Pfeffer, W. T., and N. F. Humphrey (1998), Formation of ice layers by infiltration and refreezing of meltwater, *Ann. Glaciol.*, *26*, 83–91.
- Przybylak, R. (2007), Recent air temperature changes in the Arctic, *Ann. Glaciol.*, *46*, 316–324, doi:10.3189/172756407782871666.
- Radić, V., and R. Hock (2011), Regionally differentiated contribution of mountain glaciers and ice caps to future sea-level rise, *Nat. Geosci.*, *4*, 91–94, doi:10.1038/ngeo1052.
- Rasmussen, S. O., et al. (2006), A new Greenland ice core chronology for the last glacial termination, *J. Geophys. Res.*, *111*, D06102, doi:10.1029/2005JD006079.
- Reeh, N. (1989), Parametrization of melt rate and surface temperature on the Greenland ice sheet, *Polarforschung*, *59*, 113–128.
- Santer, B. D., T. M. L. Wigley, J. S. Boyle, D. J. Gaffen, J. J. Hnilo, D. Nychka, D. E. Parker, and K. E. Taylor (2000), Statistical significance of trends and trend differences in layer-average atmospheric temperature time series, *J. Geophys. Res.*, *105*, 7337–7356, doi:10.1029/1999JD901105.
- Schaffer, N., C. Zdanowicz, L. Copland, and D. Burgess (2011), Recent volume and mass balance changes of Penny Ice Cap (Baffin Island, Nunavut) determined from repeat airborne laser altimetry, Abstract C13A-0722 presented at 2011 Fall Meeting, AGU, San Francisco, Calif., 5–9 Dec.
- Screen, J. A., and I. Simmonds (2011), Declining summer snowfall in the Arctic: Causes, impacts and feedbacks, *Clim. Dyn.*, doi:10.1007/s00382-011-1105-2, in press.
- Sepp, M., and J. Jaagus (2010), Changes in the activity and tracks of Arctic cyclones, *Clim. Change*, *105*, 577–595, doi:10.1007/s10584-010-9893-7.
- Sharp, M., D. O. Burgess, J. G. Cogley, M. Ecclestone, C. Labine, and G. J. Wolken (2011), Extreme melt on Canada's Arctic ice caps in the 21st century, *Geophys. Res. Lett.*, *38*, L11501, doi:10.1029/2011GL047381.
- Sneed, S., R. Hooke, B. Le, and G. S. Hamilton (2008), Thinning of the south dome of Barnes Ice Cap, Arctic Canada, over the past two decades, *Geology*, *36*, 71–74, doi:10.1130/G24013A.1.
- Sorterberg, A., and J. E. Walsh (2008), Seasonal cyclone variability at 70°N and its impact on moisture transport into the Arctic, *Tellus, Ser. A*, *60*, 570–586.
- Stern, H. L., and M. P. Heide-Jørgensen (2003), Trends and variability of sea ice in Baffin Bay and Davis Strait, 1953–2001, *Polar Res.*, *22*, 11–18, doi:10.1111/j.1751-8369.2003.tb00090.x.
- Tivy, A., S. E. L. Howell, B. Alt, S. McCourt, R. Chagnon, G. Crocker, T. Carrieres, and J. J. Yackel (2011), Trends and variability in summer sea ice cover in the Canadian Arctic based on the Canadian Ice Service Digital Archive, 1960–2008 and 1968–2008, *J. Geophys. Res.*, *116*, C03007, doi:10.1029/2009JC005855.
- Van De Wal, R. S. W., R. Mulvaney, E. Isaksson, J. C. Moore, J. F. Pinglot, V. A. Pojehola, and M. P. A. Thomassen (2002), Reconstruction of the historical temperature trend from measurements in a medium-length borehole on the Lomonosovfonna plateau, Svalbard, *Ann. Glaciol.*, *35*, 371–378, doi:10.3189/172756402781816979.
- Ward, W. H. (1954), Glaciological studies in the Penny Highland, Baffin Island, 1953, *Int. Assoc. Sci. Hydrol. Publ.*, *39*, 297–308.
- Ward, W. H., and P. D. Baird (1954), Studies in glacier physics on the Penny Ice Cap, Baffin Island, 1953: Part 1, A description of the Penny Ice Cap, its accumulation and ablation, *J. Glaciol.*, *2*, 342–355.
- Weaver, R. L. (1975), “Boas” Glacier (Baffin Island, N.W.T., Canada) mass balance for the five budget years 1969 to 1974, *Arct. Alp. Res.*, *7*, 279–284, doi:10.2307/1550003.
- Weber, J. R., and P. Andrieux (1970), Radar soundings on the Penny Ice Cap, Baffin Island, *J. Glaciol.*, *9*, 49–53.
- Zdanowicz, C. (2007), Glacier-climate studies on Grinnell ice cap, *Res. Rep. 012004R-M*, 37 pp., Nunavut Res. Inst., Iqaluit, Nunavut, Canada.
- Zdanowicz, C., D. Fisher, I. Clark, and D. Lacelle (2002), An ice-marginal record of $\delta^{18}\text{O}$ from Barnes ice cap, Baffin Island, Canada, *Ann. Glaciol.*, *35*, 145–149, doi:10.3189/172756402781817031.
- Zwally, H. J., and S. Fiegles (1994), Extent and duration of Antarctic surface Melting, *J. Glaciol.*, *40*, 463–476.
- Zwally, H. J., W. Abdalati, T. Herring, K. Larson, J. Saba, and K. Steffen (2002), Surface melt-induced acceleration of Greenland Ice-Sheet flow, *Science*, *297*, 218–222, doi:10.1126/science.1072708.

L. Copland and N. Schaffer, Department of Geography, University of Ottawa, Ottawa, ON K1N 6N5, Canada.

F. Dupont, Laboratoire de Glaciologie et Géophysique de l'Environnement, UMR 5183, UJF-CNRS, Grenoble F-38041, France.

J. Eley, 6 Sullivan St., Saskatoon, SK S7H 3G8, Canada.

D. Fisher and C. Zdanowicz, Geological Survey of Canada, Natural Resources Canada, 601 Booth St., Ottawa, ON K1A 0E8, Canada. (czdanowi@nrcan.gc.ca)

A. Smetny-Sowa, Department of Earth Sciences, University of Western Ontario, London, ON N6A 5B7, Canada.